Peer-reviewed version available at Molecules 2018, 23, 31; doi:10.3390/molecules23010031

Review

On the Effectiveness of Zeolite-Based Catalysts in the CO_2 Recycling to DME: State of the Art and Perspectives

Enrico Catizzone [1,*], Giuseppe Bonura [2], Massimo Migliori [1], Francesco Frusteri [2] and Girolamo Giordano [1]

[1] Dept. of Environmental and Chemical Engineering – University of Calabria – Via P. Bucci, 87036 Rende (CS), Italy; enrico.catizzone@unical.it (E.C.); massimo.migliori@unical.it (M.M.); ggiordaunical@yahoo.it (G.G.)

[2] CNR-ITAE "Nicola Giordano", Via S. Lucia sopra Contesse 5 –98126 Messina, Italy; giuseppe.bonura@itae.cnr.it (G.B.); francesco.frusteri@itae.cnr.it (F.F.)

* Correspondence: enrico.catizzone@unical.it; Tel.: +39-098-449-6669

Abstract: Starting from the environmental issues related to global warming, climate change and reduction of greenhouse gas emissions, this review paper describes how CO_2 recycling can represent a challenging strategy suitable to explore new concepts and opportunities for catalytic and industrial development. In this view, the production of dimethyl ether (DME) from catalytic hydrogenation of CO_2 appears as a viable technology, able to meet also the ever-increasing need for alternative environmentally-friendly fuels and energy carriers. Basic considerations on thermodynamic aspects controlling DME production from CO_2 are presented, then summarizing the main catalytic systems developed in such field. Special attention is paid on the role assumed during last years by zeolite-based systems, either in the methanol-to-DME dehydration step or in the one-pot CO_2-to-DME hydrogenation. On the whole, the productivity of DME results significantly to be dependent on several catalyst features, linked not only to the metal-oxide phase responsible for CO_2 activation/hydrogenation, but also to specific properties of the zeolites (i.e., topology, porosity, specific surface area, acidity, interaction with active metals, distributions of metal particles, …) influencing activity and stability of hybridized bifunctional heterogeneous catalysts.

Keywords: CO_2 hydrogenation; dimethyl ether; low-carbon processes; thermodynamics; catalysis; zeolites

1. Introduction: how can CO_2 become the future carbon source?

Carbon dioxide is recognized as the main responsible of super green-house effect causing global warming and climate change. In this concern, in order to avoid more dangerous effects, the Intergovernmental Panel on Climate Change (IPCC) and the United Nations Climate Change Conference (COP21, Paris, 2015) have emphasized the necessity to reduce carbon dioxide emissions by at least one half of current trend until 2050 aiming to limit the global average temperature increase to a maximum of 2 °C [1]. Carbon dioxide is mainly emitted from power plants (e.g. coal-based) and cars but also other industrial sources, such as boilers or cement and steel plants contribute to increase the emission of carbon dioxide into the atmosphere [2].

During the last decades, several strategies and technologies have been developed concerning capture and storage of carbon dioxide (CCS) and by 2020 the number of projects concerning this aspect is expected to double even if few large-scale CCS plants are at present realized [2]. On the other hand, during the last years, the scientific community agrees to consider CO_2 not a waste and a

cost (especially in the countries where carbon taxes are applied) but a carbon source of the future in alternative to the fossil ones. Therefore, the future perspectives about reduction on carbon dioxide emissions will not only concern the development of more efficient technologies for CCS but especially the conception of new strategies able to convert carbon dioxide to fuels and energy. The most interesting strategy, well-known as Methanol Economy Theory introduced by Nobel Laureate George A. Olah, bases on the fact that the actual carbon- and energy-sources (e.g. oil, coal, natural gas) can be replaced by methanol [3]. In fact, methanol can be readily converted in several high-value products that can be used for both energy or chemicals production. Methanol-to-Olefin process (MTO) is a promising technology able to convert methanol into ethylene and propylene, the main basic building blocks for polymer industry (e.g. production of PE or PP). More details about this process are reported by Tian *et al.* [4]. Briefly, this process is usually carried out in a fluidized bed reactor operating with low partial pressure of methanol, in the temperature range 400-450 °C and using SAPO-34-type zeolite as catalyst. Adopting slightly lower temperature (about 350 °C), higher pressure (about 30 bar) and medium-pore zeolites such as ZSM-5, methanol is converted into gasoline-cut hydrocarbons (Methanol-to-Gasoline process, MTG) [5]. Despite certainly methanol can be considered an interesting molecule for the industrial chemistry it cannot be considered a safe molecule due its toxicity being, therefore, a potential risk for population its large use. All of the above mentioned processes involve dimethyl ether (DME) as intermediate that can be easily obtained by dehydration of methanol as detailed below.

DME, the simplest of ether, is a neither toxic nor carcinogenic molecule with a boiling point of -25°C but it can be liquefied above 0.5 MPa at room temperature [6]. Chemical and physical properties of DME are similar to those of LPG, and published studies suggested that the technologies developed for storage and transport of LPG can be easily converted to accommodate DME with similar safety guidelines and codes [7]. DME is also an important chemical intermediate for production of widely used chemicals, such as diethyl sulphate, methyl acetate and, as mentioned before, light olefins and gasoline [8]. Nowadays, DME is mainly used as an aerosol propellant in several spray cans, replacing the banned ozone-destroying CFC compounds but in the last decades, it is receiving a growing attention as an alternative eco-friendly fuel. In 1995, an extensive collaborative research effort among Amoco (actual BP), Haldor Topsoe and Navistar International Corporation, demonstrated that DME could be a reliable alternative fuel for diesel engines with low-emission of NOx, SOx and particular matter, to be produced at large-scale from methanol by a simple dehydration technology [9]. These studies renewed attention on the outstanding performances of DME as alternative fuel to diesel and showed total compliance with the most stringent California ULEV (ultra-low emission vehicle) emission regulations for medium-duty vehicles. Because of the necessity to change the fuel distribution infrastructures and the modifications to engine devices, DME market as diesel alternative fuel is still an open challenge. Indeed, the primary DME market was the blending of DME with LPG and Amoco patented a DME/LPG blend for automotive applications [10]. The current key market perspectives of use of DME as fuel are: 1) blending with LPG; 2) alternative fuel for diesel engines; 3) fuel for power generation in gas turbine plants; 4) chemical intermediate for olefins and synthetic gasoline production. Therefore, rather than methanol, dimethyl ether can be considered as reliable energy vector of the future and as chemical intermediate in low-carbon processes. In this concern, carbon dioxide can be used as reactant to produce methanol and then DME. The most

studied way to produce methanol is the hydrogenation of carbon dioxide according to the following reaction:

$$CO_2 + 3H_2 = CH_3OH + H_2O$$

and DME as product of dehydration of the alcohol:

$$2CH_3OH = CH_3OCH_3 + H_2O$$

By considering the reverse water shift reaction:

$$CO_2 + H_2 = CO + H_2O$$

the global reaction leads formation of DME is the following:

$$2CO_2 + 6H_2 = CH_3OCH_3 + 3H_2O$$

As stoichiometric suggests, six moles of hydrogen are required to produce one mole of DME. Since hydrogen is usually produced from fossil hydrocarbons (e.g. steam reforming of natural gas), there are no real advantages to use this way to produce DME or methanol via CO_2 hydrogenation. Therefore, only if hydrogen is produced starting from non-fossil sources, the Methanol/DME Economy Theory could be applied; in particular, if hydrogen is directly produced using renewable energy sources, carbon dioxide hydrogenation towards fuels/energy vectors (e.g. DME) became a valuable strategy for a reliable utilization of renewable energy in both chemical industrial and power generation. Hydrogen can be produced from renewables following several ways. The current approach is the production of electrical energy by using renewable energy sources (e.g. solar energy) and the use of this energy for electrolysis of water using PEM cells [11]. Beside this route, other approaches were examined such as production of hydrogen from cyanobacteria or algae [12, 13], biomass thermos-chemical process or anaerobic fermentation [14, 15] or direct production of H_2 by water photo-electrolysis [16, 17]. Therefore, this attractive closed carbon cycle can be summarized in five steps as it follows (see also Figure 1):

a) Production of hydrogen via water splitting by using renewable energy (e.g. solar energy);

b) Capture and safe storage of CO_2 emitted from power plants or from atmosphere;

c) Hydrogenation of CO_2 available from step (b) with hydrogen produced in step (a) to produce methanol and/or dimethyl ether (DME should be preferable to MeOH because its no-toxicity as discussed above);

d) Utilization of DME as fuel for production of energy or as intermediate in the chemical chain industry;

e) Reuse the carbon dioxide from eco-friendly combustion of DME to re-produce its self.

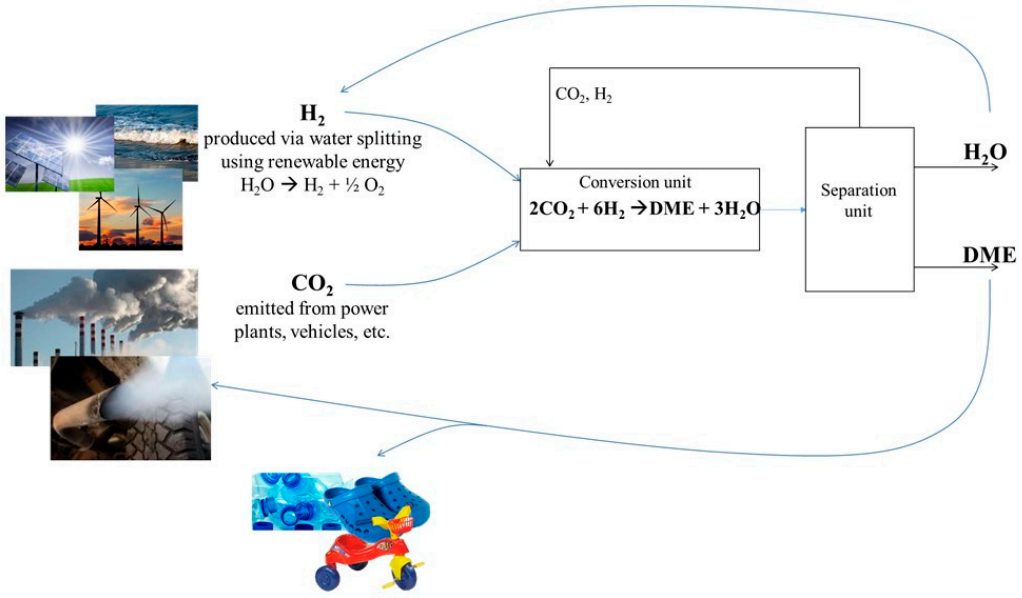

Figure 1. Proposed closed carbon cycle involving DME as energetic vector.

Following this strategy and growing research effort on each of the above mentioned steps will be possible to create an efficient CO_2-based production system for both chemicals and energy aiming to meet both energy security (by reducing the dependence on fossil sources) and socio-environment security (by reducing the carbon dioxide emissions into the atmosphere) [11]. Among the several challenges concerning the practical application of the above described attractive strategy, the development of a high efficient catalyst for CO_2 hydrogenation is still an open challenge despite several works have been carried out during the last years. Since the formation of DME via one-pot CO_2 hydrogenation involves two reaction steps, e.g. methanol formation and methanol dehydration, the catalyst should exhibit a redox function able to hydrogenate CO_2 to alcohol and an acid function able to convert the alcohol in the ether. Several strategies have been proposed in order to prepare a catalyst able to produce DME via one-pot hydrogenation of CO_2 with good performances in terms of CO_2 conversion, DME selectivity and stability. Recently, Álvarez *et al.* [18], discussed some catalytic aspects concerning one-pot CO_2-to-DME process, revealing that further advances in research are necessary in order to develop a high active catalyst. In fact, despite Cu-based catalyst is expected to remain the most efficient catalyst for CO_2-to-methanol reaction step, some aspects about bifunctional catalyst such as (i) the choice of the acid function, (ii) the method used to prepare hybrid catalyst, (iii) copper particle sintering and (iv) catalyst deactivation remain the main open challenge in view of an optimization of the process.

This paper, after a brief discussion about the use of DME as alternative fuel and thermodynamics of CO_2-to-DME process, will focus on the critical evaluation of catalytic systems proposed up to now devoting particular attention to the effect of both physicochemical properties of redox and acid functions and the preparing method on catalytic performances of hybrid catalyst emphasizing on the potential of zeolites as efficient acid catalysts for methanol dehydration step.

2. DME as valuable fuel of the future

As reported in the previous paragraph, since the middle of 1990s DME has been promoted as a reliable diesel substitute for auto-transportation and chemical-physical properties comparison between diesel fuel and DME is reported in Table 1, allowing to identify both advantages and disadvantages of using DME as alternative fuel for diesel engines.

Table 1. Physicochemical properties of DME and diesel fuels [6]

	Unit	DME	Diesel
Carbon content	mass%	52.2	86
Hydrogen content	mass%	13	14
Oxygen content	mass%	34.8	0
Carbon-to-hydrogen ratio	-	0.337	0.516
Liquid density	kg/m3	667	831
Cetane number	-	>55	40-50
Autoignition temperature	K	508	523
Stoichiometric air/fuel mass ratio	-	9.6	14.6
Normal boiling point	K	248.1	450-643
Enthalpy of vaporization	kJ/kg	467.1	300
Lower heating value	MJ/kg	27.6	42.5
Ignition limits	vol% in air	3.4/18.6	0.6/6.5
Modulus of elasticity	N/m2	6.37·108	14.86·108
Liquid kinematic viscosity	cSt	<0.1	3
Surface tension (at 298K)	N/m	0.012	0.027
Vapour pressure (at 298 K)	kPa	530	<<10

The lower boiling point, leads to a faster evaporation when liquid DME is injected into the engine cylinder improving the combustion. In addition, the lower auto-ignition temperature allows to obtain a higher cetane number of DME than that exhibited from diesel fuel. Generally, a higher cetane number results in easier ignition, more complete combustion and cleaner exhausted gases; in addition, a higher cetane number of fuel allows to reduce the smoke emission during engine warm-up, to reduce noise and to reduce both fuel consumption and exhausted gas emissions [6, 19]. In addition, based on the similar chemical-physical properties between DME and LPG, several devices as the storage bottle and fuel line used in LPG-based systems can be used for DME.

On the other hand, some disadvantages have to be accounted to fulfil evaluation of DME as substitute of diesel. First of all, DME exhibits a LHV much lower than diesel fuel (27.6 MJ/kg vs 42.5 MJ/kg) and for this reason a larger amount of injected volume and longer injection period for DME is necessary in order to deliver the same amount of energy. Other disadvantages are related to necessity to change engine configuration if diesel fuel is substituted with DME fuel. In fact, the lower viscosity of DME requires the application of special gaskets in order to avoid fuel leakages. In addition, DME is able to dissolve organic compounds and it is not compatible with elastomers and plastic materials. Therefore, a careful selection of sealing materials is also required when DME is used as fuel in diesel engines [20]. The diesel-fueled compression ignition (CI) engine offers several

advantages compared to a gasoline-fueled spark ignition (SI) engine (e.g. better fuel economy, higher power performances, and expected life). Nevertheless, CI engine has several well-known disadvantages. Because the higher combustion chamber temperature and the chemical-physical characteristics of diesel fuel, harmful pollutants such as nitrogen oxides (NOx), particular matter (PM), hydrocarbon compounds (HC), carbon monoxide (CO) and sulphur oxides (SOx) are emitted. As reported by Park *et al.* [20], emissions of HC and CO are lower if DME is burned in a CI engine and the absence of sulphur in DME fuel, allows to obtain SOx-free exhausted gases. Formation of particular matter (soot) is typical of diesel-fueled compression-ignition engines causing the necessity to use an anti-particulate filter (APF) in order to reduce that emissions. The high oxygen content and the absence of C-C bonds in DME molecule does not favor formation of soot during combustion eliminating the just described problem associated to diesel fuel. Experimental results reported by Sidhu *et al.* [21] show that the relative particulate yields from DME was just 0.026% versus the value of 0.51% exhibited from both diesel and bio-diesel fuels. For this reason, an APF is not required in DME-fueled engines. Thanks to this advantage, installation and application of oxidation catalysts for further reduction of both HC and CO is possible in terms of economy and vehicle space.

A right evaluation and comparison of NOx emission from CI engines by using DME or diesel fuel is not easy to perform experimentally because results strongly depend on the engine conditions and the fuel supply system. Usually, a higher NOx level was detected when diesel fuels is substituted with DME, as reported be Park *et al.* and Kim *et al.* [20, 22] but opposite results have been published by SAE International studies [23, 24]. Unlike diesel fuel, the reduced emission of the other pollutants, allows to use high exhaust gas recirculation (EGR) in order to reduce NOx level without an increase in PM and soot emissions [19].

On the other hand, not only combustion performances have to be accounted of when assessing the possibility to use a substance as alternative fuel. In fact, a carefully evaluation on the efficiency of each step, from the supplying of raw material to utilization of the final fuel is required. In this concern, a well-to-wheels (WTW) analysis is usually performed. A well-to-wheels analysis consists of a well-to-tank (WTT) and a tank-to wheels (TTW) analysis [19]. The WTT analysis can be carried out by calculating the WTT efficiency as the ratio between the energy of the fuel (e.g. in terms lower heat value LHV) and the sum of the energy consumptions in each manufacturing step, from feedstock recovery to fuel distribution. Among the derived alternative fuels from natural gas, biomass or electrolysis (e.g. DME, methanol, synthetic diesel, hydrogen, etc.), DME exhibits the highest WTT efficiency [19]. TTW analysis includes everything related to the vehicle and its characteristics and for these reason different fuels have to be compared for same engine technology. In this context, DME exhibits high engine efficiency for several vehicle technologies. Globally, by comparing WTT and TTW analysis in order to estimate a WTW efficiency, Semelsberg *et al.* [19] according to Arcoumanis *et al.* [6], suggest that DME ranks on the top among different alternative fuel for several vehicle technologies. The WTW efficiency of DME is comparable with LPG and CNG (compressed natural gas) fueled vehicles, but lower than vehicle operating with diesel fuel.

Because of the clean emission offered from DME combustion, DME is also suggested as fuel for power generation by using gas turbines. In the last decade, several companies, including BP, Snamprogetti/ENI S.p.A, Haldor Topsoe [25], have tested DME as a gas turbine fuel in the case that they cannot easily import natural gas. In fact, as above mentioned, thanks to the similar chemical-physical properties of DME and LPG, ocean transport can be carried out by using conventional LPG

tankers without any additional precautions about both safety and technologies. Several studies demonstrate that DME is a reliable, clean, fuel compared with natural gas in terms of both NOx and CO [26, 27]. Depending on operation conditions, DME can emits more CO than NOx [28] but this disadvantage can be overcoming by slight modification of nozzles [29].

As discussed in the introduction part, hydrogen generation is a key point of the proposed future CO_2-based scenario involving DME as energy vector [30, 31]. Production of hydrogen by steam reforming of methane or gasoline is the main industrial process to produce hydrogen. These processes require high temperature (above 600 °C for methane and above 800 °C for gasoline), high energy supply, stable catalysts and expensive refractory reactors. Recently, steam reforming of methanol is receiving attention because relative low process temperature (around 300°C) and simpler reactor configurations [32]. Nevertheless, because the high toxicity of methanol, DME is considered reliable candidate even for hydrogen production by steam reforming (by adopting similar operation condition of methanol steam reforming and over a bi-functional catalyst, namely acid function of DME hydrolysis to methanol and copper-based catalyst for the alcohol reforming) because it is not toxic and because its high hydrogen content, as it was confirmed by several studies [33-36].

3. Thermodynamic considerations on CO_2-to-DME process

CO_2 hydrogenation to DME usually involves four reactions summarized in Table 2.

Table 2. List of reactions involved in one-pot CO2 hydrogenation to DME.

Reaction No.	Reaction stoichiometry	$\Delta\tilde{H}^{\circ}_{298\ K}$
1	$CO_2 + 3H_2 = CH_3OH + H_2O$	-49.5 kJ/mol$_{CO2}$
2	$2\ CH_3OH = CH_3OCH_3 + H_2O$	-23.4 kJ/mol$_{DME}$
3	$CO_2 + H_2 = CO + H_2O$	+41.2 kJ/mol$_{CO2}$
4	$CO + 2H_2 = CH_3OH$	-90.6 kJ/mol$_{CO}$

For all of the involved reactions it is possible to calculate equilibrium constants as follows:

$$K_j(T) = \prod_i a_i^{\nu_{ij}} = \exp\left(\frac{-\Delta\tilde{G}_{rj}}{RT}\right)$$

where a_i is the activity of specie *i* involved in the reaction *j* with the stoichiometric number ν_{ij} while $\Delta\tilde{G}_{rj}$ is the molar Gibbs energy change of reaction *j* that can be calculated as it follows:

$$\Delta\tilde{G}_{rj} = \sum_i \nu_{ij}\tilde{G}_i\ (T, P)$$

Since all species are in gaseous phase a state standard activity of pure gas at 1 bar can be chosen as reference to compute activity as it follows:

$$a_i = \frac{\bar{f}_i}{1\,bar}$$

where $\bar{f}_i$ is the fugacity of specie *i* in the gaseous mixture that has been computed adopting Peng-Robinson equation of state.

Therefore, the equilibrium constants can be expressed as follows:

$$K_1(T) = \frac{\bar{f}_{CH_3OH} \cdot \bar{f}_{H_2O}}{\bar{f}_{CO_2} \cdot \bar{f}_{H_2}^2} = \exp\left(\frac{-\Delta\tilde{G}_{r1}^0(T)}{RT}\right)$$

$$K_2(T) = \frac{\bar{f}_{CH_3OCH_3} \cdot \bar{f}_{H_2O}}{\bar{f}_{CH_3OH}^2} = \exp\left(\frac{-\Delta\tilde{G}_{r2}^0(T)}{RT}\right)$$

$$K_3(T) = \frac{\bar{f}_{CO} \cdot \bar{f}_{H_2O}}{\bar{f}_{CO_2} \cdot \bar{f}_{H_2}} = \exp\left(\frac{-\Delta\tilde{G}_{r3}^0(T)}{RT}\right)$$

$$K_4(T) = \frac{\bar{f}_{CH_3OCH_3}}{\bar{f}_{CO_2} \cdot \bar{f}_{H_2}^2} = \exp\left(\frac{-\Delta\tilde{G}_{r4}^0(T)}{RT}\right)$$

The mass balance on specie i can be wrote as following:

$$n_i^{eq} = n_i^0 + \sum_j \nu_{ij}\xi_j$$

where n_i^{eq} and n_i^0 are the final and the initial moles of specie *i*, respectively and ξ_j is the progress grade of reaction *j*.

Accordingly, the CO_2 equilibrium conversion can be calculated as follows:

$$X_{CO_2} = \frac{n_{CO_2}^0 - n_{CO_2}^{eq}}{n_{CO_2}^0} = \frac{\xi_1 + \xi_3}{n_{CO_2}^0}$$

while selectivity on C-basis towards DME, MeOH and CO according to the following equations:

$$S_{DME} = \frac{2 \cdot \xi_2}{\xi_1 + \xi_3}$$

$$S_{MeOH} = \frac{\xi_1 + \xi_4 - \xi_2}{\xi_1 + \xi_3}$$

$$S_{CO} = \frac{\xi_3 - \xi_4}{\xi_1 + \xi_3}$$

Simulation was performed using Unisim Design R430 (Honeywell) software imposing an initial reactant mixture composed only by CO_2 and H_2. In this paragraph, the effect of reaction parameters such as reaction temperature, reaction pressure and inlet H_2/CO_2 ratio on thermodynamics of one-pot CO_2 hydrogenation to DME are discussed.

Figure 2 reports the equilibrium theoretical conversion of CO_2 as a function of reaction temperature and reaction pressure estimated imposing an initial H_2/CO_2 ratio equals to 3 mol_{H2}/mol_{CO2}.

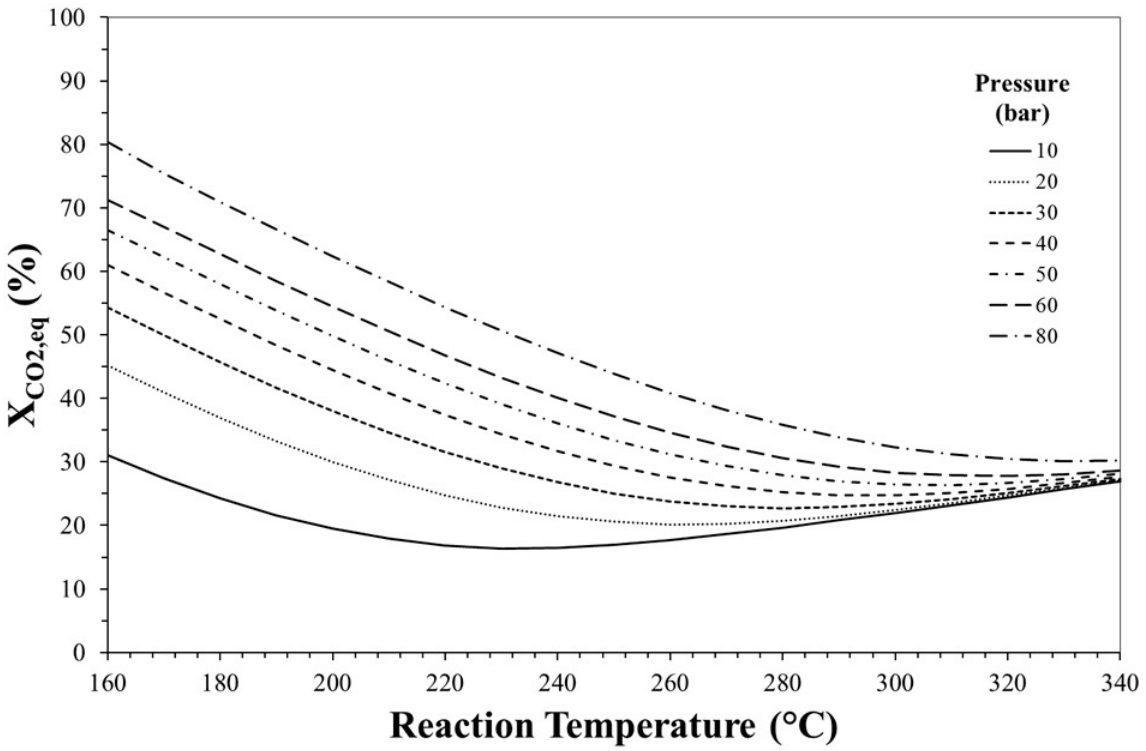

Figure 2. Effect of reaction temperature and pressure on CO_2 equilibrium theoretical conversion. Initial H_2/CO_2 molar ratio equals to 3.

The increase in reaction pressure promotes CO_2 conversion since global reaction proceeds with a decrease in the number of moles even if this effect slights at high temperature. For instance, at 160 °C, $X_{CO2,eq}$ rises from ca. 30% to ca. 80% by increasing the reaction pressure from 10 bar to 80 bar, while at higher temperature, e.g. 340 °C, the increase in $X_{CO2,eq}$ can be considered negligible.

On the contrary, since the process involves both exothermic (i.e. step (1), (2) and (4), see Table 2) and endothermic (i.e. step (3), see Table 2) reactions, the effect of increase in temperature on CO_2 equilibrium conversion is disadvantageous at low temperature and advantageous at high temperature, even if this effect is more marked at low pressure. For instance, at 10 bar, $X_{CO2,eq}$ decreases from ca. 30% to ca. 16% when the temperature increases from 160 °C to 230°C and it increases to ca. 28% if the reaction temperature rises to 340 °C, suggesting that at high temperature reverse water gas shift reaction that also favor CO_2 consumption predominates over the other steps.

Figures 3, 4 and 5 show the effect of reaction temperature and pressure on selectivity towards DME, CO and methanol, respectively.

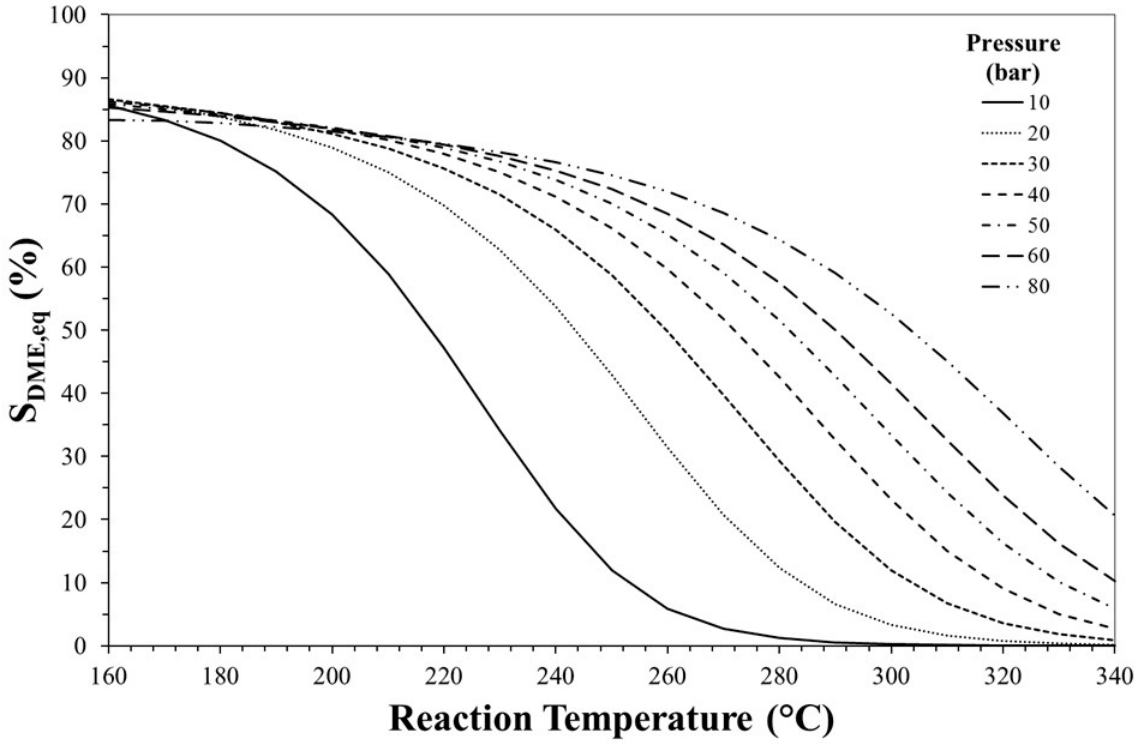

Figure 3. Effect of reaction temperature and pressure on DME equilibrium theoretical selectivity. Initial H_2/CO_2 molar ratio equals to 3.

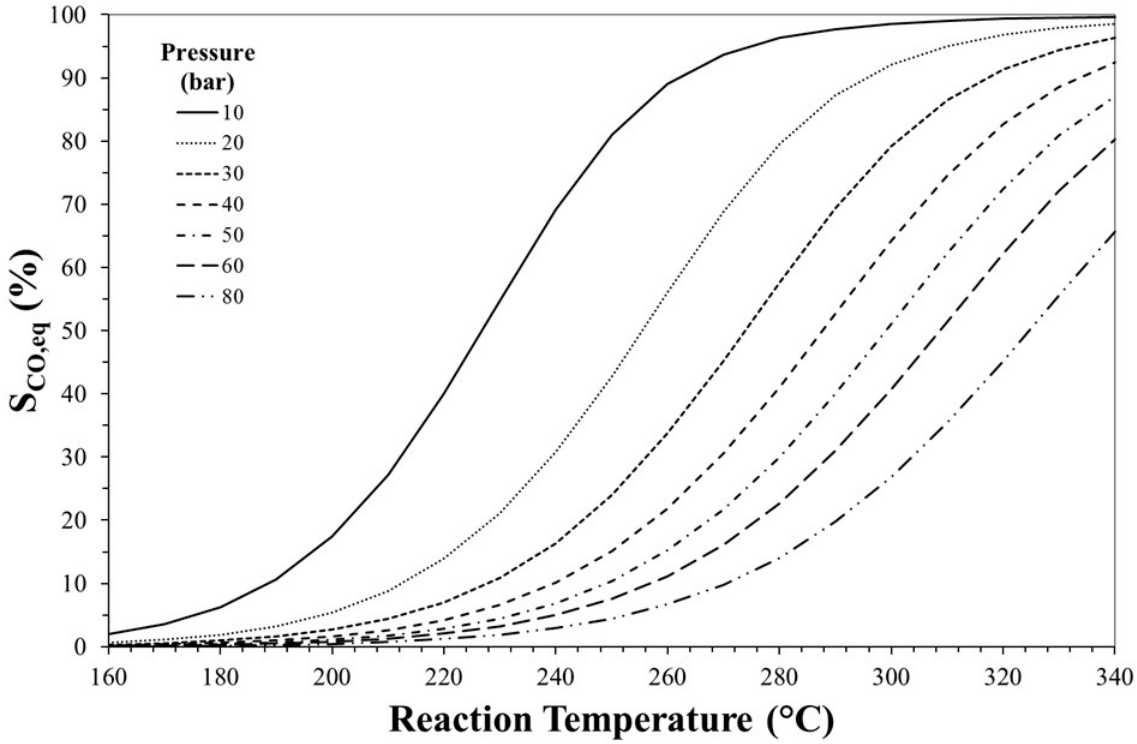

Figure 4. Effect of reaction temperature and pressure on CO equilibrium theoretical selectivity. Initial H_2/CO_2 molar ratio equals to 3.

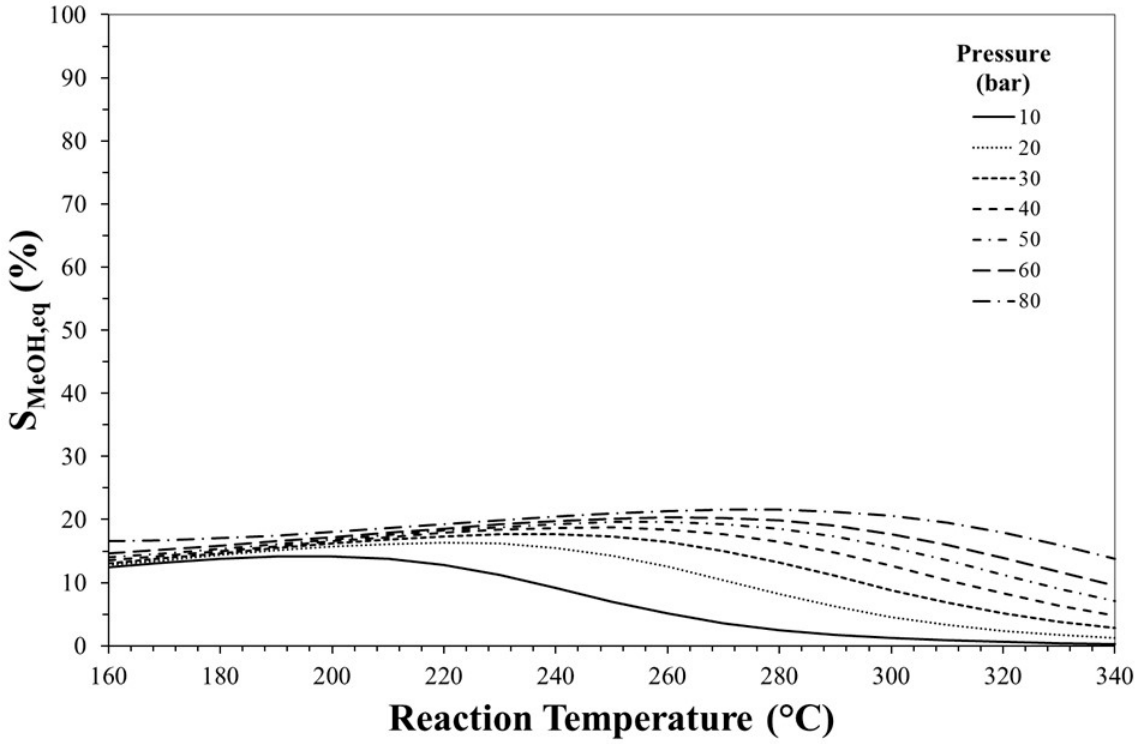

Figure 5. Effect of reaction temperature and pressure on methanol equilibrium theoretical selectivity. Initial H_2/CO_2 molar ratio equals to 3.

As mentioned before, low temperature should be adopted in order to favor exothermic reactions achieving high DME selectivity. In fact, high temperatures favor rWGS promoting CO formation and lowering selectivity towards DME.

Especially at high temperature, DME selectivity can be improved by increasing the reaction pressure. For instance, at 240 °C, DME equilibrium selectivity can be increased from ca. 20% to ca. 60% by pressuring the system from 10 bar to 30 bar while selectivity towards CO can be reduced from ca. 70% to values below 20%.

The equilibrium selectivity towards methanol is favored by high pressure and low temperature even if it can be estimated always lower than 20%.

Also reactant mixture composition strongly affects process thermodynamics as shown in Figure 6.

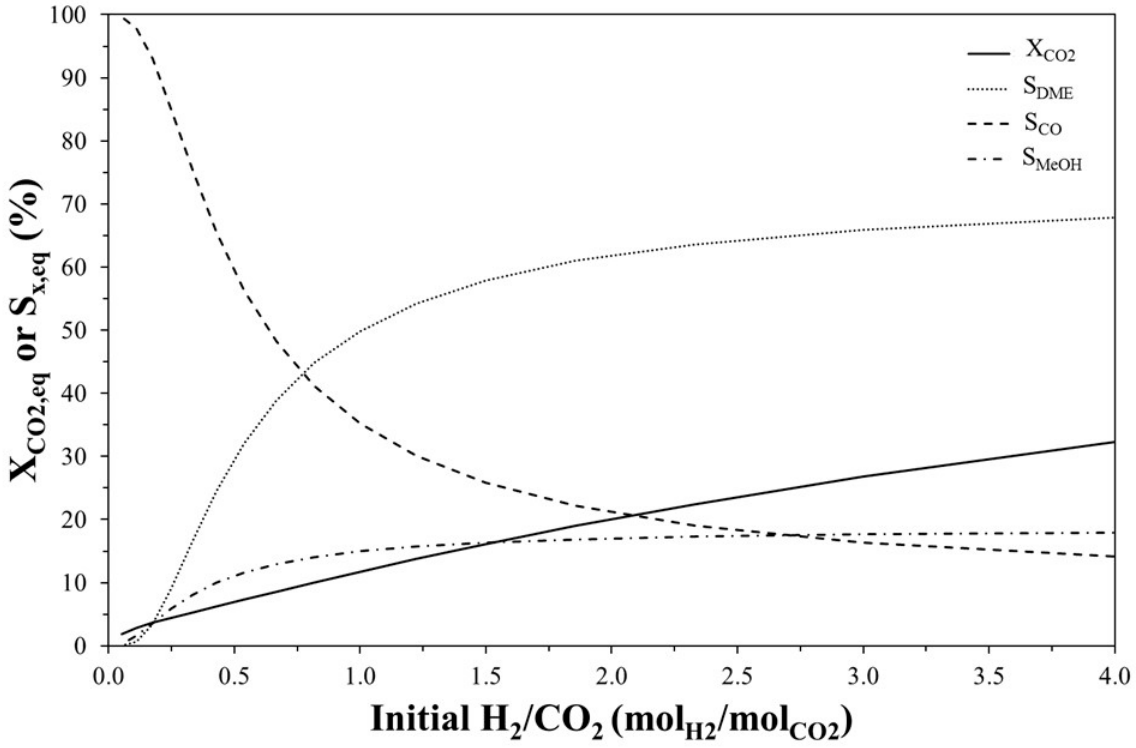

Figure 6. Effect of initial H_2/CO_2 molar ratio on CO_2 equilibrium conversion and DME, CO and methanol equilibrium selectivity. Reaction temperature and pressure: 240 °C and 30 bar, respectively.

Increasing the H_2/CO_2 molar ratio in the feedstock improves CO_2 conversion and a H_2/CO_2 value higher than 0.8 mol_{H2}/mol_{CO2} (at 240 °C and 30 bar) should be adopted in order to obtain a selectivity towards DME higher than that towards CO. In fact, high CO_2 concentration favors CO formation from rWGS causing a DME selectivity loss. On the contrary, high DME selectivity values can be predicted for high H_2 initial content even if the effect is more pronounced at low H_2/CO_2 ratio.

3.1 The effect of methanol dehydration reaction step on thermodynamics

It is well known that DME production from CO_2 can be carried out in a two-step process in which methanol is produced via CO_2 hydrogenation in a first reactor, purified and then dehydrated to produce DME in another reactor while on one-pot process both of the reaction steps are carried out in a single reactor [37]. Figure 7 shows the effect of temperature and pressure on CO_2 conversion for both one-step and two-step process.

Preprints (www.preprints.org) | NOT PEER-REVIEWED | Posted: 11 November 2017 doi:10.20944/preprints201711.0071.v1

Peer-reviewed version available at Molecules 2018, 23, 31; doi:10.3390/molecules23010031

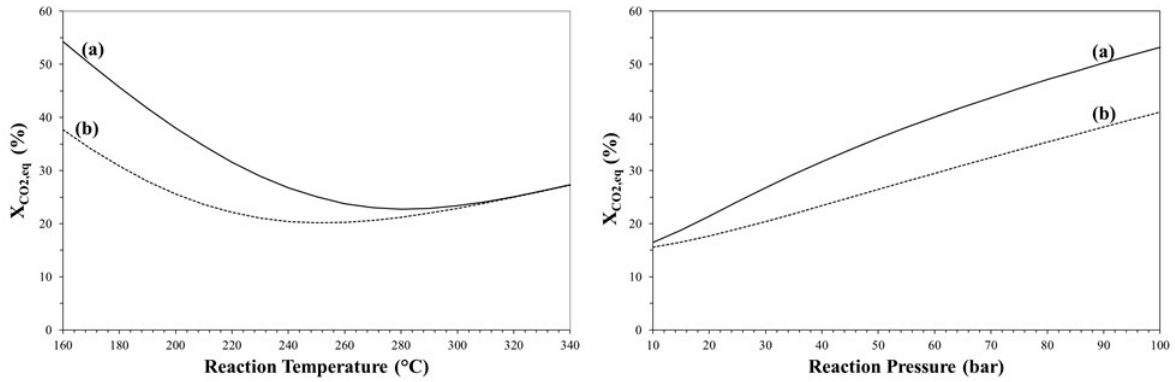

Figure 7. CO_2 equilibrium theoretical conversion of CO_2-to-DME (a) and CO_2-to-MeOH (b) process as a function of reaction temperature (left) and pressure (right).

As consequence of methanol consumption by dehydration reaction (2), one-step process is more efficient than two-step process in terms of CO_2 equilibrium conversion, even if this thermodynamic benefit is more valuable at low temperature and high pressure.

In order to quantify the thermodynamic benefit of using one-pot process CO_2 conversion percentage gain CPG can be calculated as it follows:

$$CPG = \frac{X^{a}_{CO_2,eq} - X^{b}_{CO_2,eq}}{X^{b}_{CO_2,eq}} \cdot 100$$

where $X^{a}_{CO_2}$ and $X^{b}_{CO_2}$ are the CO_2 equilibrium conversion predicted for one-step or two-step process, respectively.

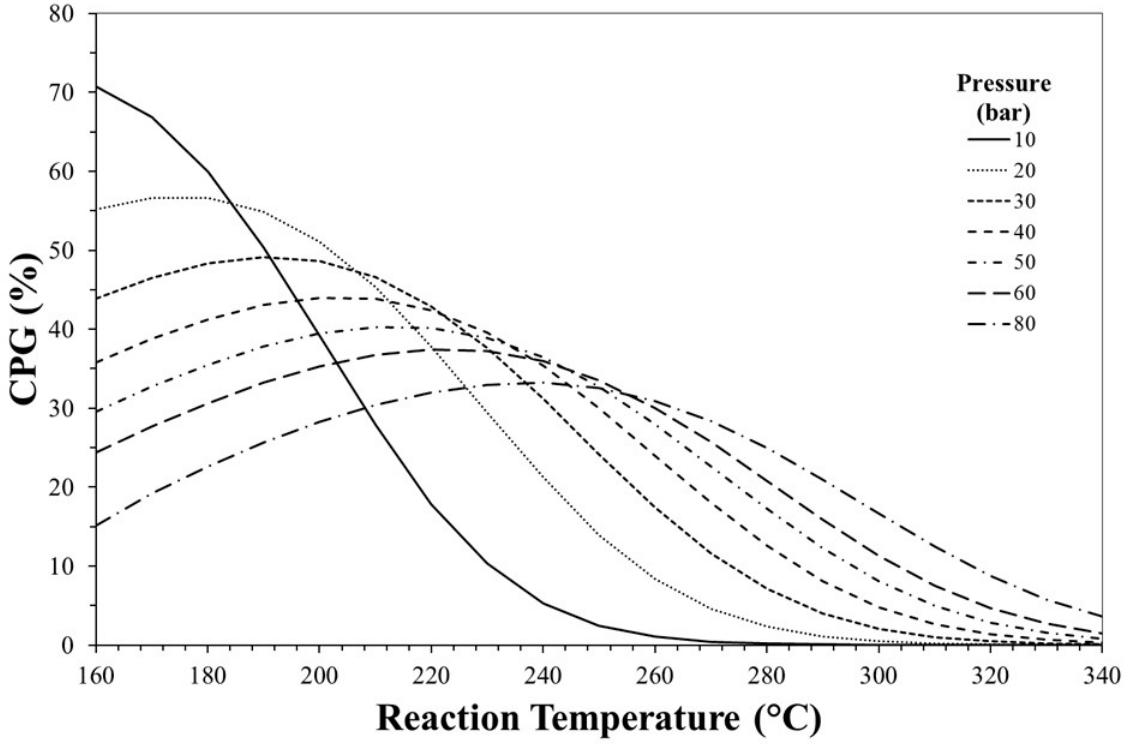

Figure 8. CO_2 conversion percentage gain (CPG) as a function of reaction temperature and pressure

Figure 8 reports CPG as a function of reaction temperature and pressure. The obtained graph can be used as a tool to individuate the optimal operation conditions to have the maximum thermodynamic benefit in terms of CO_2 conversion via the direct process. For instance, at reaction pressure of 30 bar, the maximum benefit in terms of X_{CO2} to carry out one-step rather than two-step process can be obtained at ca. 200 °C.

4. Catalytic systems for DME production

As mentioned before, DME synthesis could be performed in either a two-step process (indirect synthesis) or a single-step process (direct synthesis) [38]. In the conventional indirect synthesis, methanol is first synthesized on a metallic-based catalyst through COx hydrogenation [39], then, methanol is dehydrated into DME over solid acid catalysts, such as γ-alumina, zeolite, heteropolyacids and so on. On the other hand, the direct DME synthesis is an attractive alternative to the two-step process [40-42], in which the catalyst functionalities of methanol synthesis and in-situ dehydration are integrated in bifunctional systems within a single reactor (see Figure 9), so alleviating the thermodynamic constraints of methanol synthesis and leading to higher CO_2 conversion and higher DME selectivity [38, 39, 43].

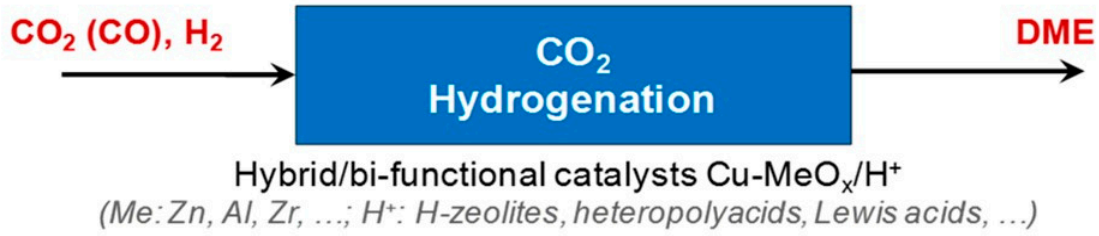

Figure 9. Scheme of the direct synthesis of DME through CO2 hydrogenation.

Moreover, from an industrial point of view, the use of a single reactor should reduce the capital costs for the DME production [44-46].

It is also important to mention that the real direct DME synthesis product distribution may not correspond to the predicted values by thermodynamics. The product distributions are also controlled by kinetics, although a good understanding of the thermodynamic limitations for direct DME synthesis reaction can be useful for developing new chemical processes and improving old ones (see Paragraph 3). Anyway, the indirect synthesis has been dominant for most of the world DME production [47]. Whatever the process, catalyst features strongly affect process performances such as product distribution and deactivation of the catalyst. In this paragraph, the effect of both metal or acid catalyst properties on DME production are discussed emphasizing the potential of zeolites as acid catalysts.

4.1 Catalysts for CO_2-to-MeOH step

In literature several catalytic systems are claimed as active in the activation of carbon dioxide. Table 3 lists the best performing catalysts together with the active species used (Cu, Ag, Au, Ni, Pd, Pt), the preparation method and their respective physicochemical and morphological properties [47].

Table 3. Textural and catalytic properties of metal/zirconia catalysts (Reproduced from [47] with permission of The Royal Society of Chemistry).

Catalyst M/ZrO_2	Prep.[a]	Precursors	BET surface/ $m^2\ g_{cat}^{-1}$	Metal surface/ $m^2\ g_{cat}^{-1}$	Product selectivity[b]			Ref.
					CH_3OH	CO	CH_4	
Cu	impreg.	Copper formate	–	–	–	–	–	11–13
Cu	impreg.	Copper tetrammine	107	1.8	35	65	0	14
Cu	co-prec.	Nitrates	64	–	68	32	0	15, 16
Cu	co-prec.	Nitrates	174	7.1	66	34	0	14, 17
Cu	co-prec.	Chloride/ Sulfate	48.4	–	53	47	0	18
Cu	ho-prec.	Nitrates	161	3.0	69	31	0	17
Cu	prec.	Nitrates	86	–	15	57	28	19
Cu	sol–gel	Acetate	215	–	40	60	0	20
Cu	alloy	$Cu_{70}Zr_{30}$	47	5.0	64	36	0	21
HT-Cu	sol–gel, 2	Acetate	128	0.8	100–55			22
HT-Cu	sol–gel, 1	Acetate	100	–	100–55			22
HT-Cu	sol–gel, 1	HNO_3	143	1.3	100–55			22
LT-Cu	sol–gel, 1	HNO_3	139	5.0	100–55			22
Cu/CZ1	sol–gel		253	–	52	47		23
Cu/CZ2	sol–gel		268	17.8	96	4		23
Cu/CZ3	sol–gel		241	28.5	97	3		23
Cu/CZ4	sol–gel		234	31.3	97	3		23
Cu/CZ5	sol–gel		225	41.2	96	4		23
Cu/ZnO	sol–gel	Acetates	150	–	64	36	0	20
Cu/ZnO 01	ox-co-prec.	Nitrates	39	3.4	36/40			24
Cu/ZnO 02	ox-co-prec.	Nitrates	36	14.9	37/46			24
Cu/ZnO 03	ox-co-prec.	Nitrates	70	12.6	38/42			24
Cu/ZnO 04	ox-co-prec.	Nitrates	45	9.6	37/43			24
Cu/ZnO 05	carb-co-prec.				33/38			24
Cu/V	prec.	Nitrates	185	–	13	67	20	19
Cu/Ag	co-prec.	Nitrates	281	4.1	81	19	0	25
Ag	co-prec.	Nitrates	112	–	100	0	0	25
Ag	impreg.	Nitrates	125	–	70	30	0	26
HT-Ag	sol–gel, 2	Acetate	99	–	100–55			22
HT-Ag	sol–gel, 1	Acetate	77	–	100–55			22
HT-Ag	sol–gel, 1	HNO_3	125	–	100–55			22
LT-Ag	sol–gel, 1	HNO_3	112	–	90–48			22
Au	co-prec.	$HAuCl_4$/ $ZrO(NO_3)_2$	185	–	24	76	0	26, 27
Au	alloy	$Au_{25}Zr_{75}$	47	–	20	74	6	27
Pt	impreg.	$HPtCl_6$/ chloride	–	–	5	2	93	28
Pd	alloy	$Pd_{33}Zr_{67}$	17	5.6	30	27	43	29
Ni	alloy	$Ni_{64}Zr_{36}$	8	–	0	0	100	30
Rh	impreg.	Nitrate/ chloride	–	–	5	32	63	31
Rh	impreg.	Nitrate chloride	–	–	0	0	100	32, 33
Ru	impreg.	Ru(III)AcAc	–	–	0	0	100	34
Re	impreg.	–	–	4.1	11	58	29	35
Rh–Mo	impreg.	Molybdate/ chloride	54		0		100	36
Rh–Mo–Li	impreg.	Molybdate/ chloride/ nitrate	47		0		100	36
Rh–Mo–K	impreg.	Molybdate/ chloride/ nitrate	51		0		100	36
Rh–Mo–Re	impreg.	Molybdate/ chloride/ perrhenate	52		0		100	36
Rh–Mo–Co	impreg.	Molybdate/ chloride/ nitrate	53		0		100	36
Rh–Mo–Ce	impreg.	Molybdate/ chloride/ nitrate	57		0		100	36

[a] Alloy: controlled oxidation of amorphous alloys, co-prec.: co-precipitation, impreg.: impregnation, ho-prec.: homogeneous precipitation using urea, sol–gel, 1/2: one/two stage sol–gel methodology, ox-co-prec: oxalate co-precipitation, carb-co-prec: carbonate co-precipitation. [b] Note: product selectivities were obtained under different experimental conditions.

Among these, copper-based catalysts exhibit the best catalytic performance in terms of CO_2 hydrogenation to methanol. In addition, previous studies identified the following order of catalytic activity [48]:

$$Cu >> Co = Pd = Re > Ni > Fe >> Ru = Pt > Os > Ir = Ag = Rh > Au$$

On the whole, this reactivity trend confirms that copper-based systems are the most active ones in the CO_2 activation. In any case, it must be said that catalytic activity heavily depends on metal dispersion, the use of dopants, and the choice of the support. A further key point regarding catalytic hydrogenation from CO_2 rather than syngas is related to the higher oxidation power of CO_2 with respect to CO, thus influencing the active state of the catalyst for methanol synthesis and consequently the formation rate of methanol [49]. Therefore, there is a strong influence of the reaction conditions on the overall catalytic behavior and the need to develop appropriate kinetic models to describe the overall synthesis. This is the basis for a proper modeling of the process and its optimization.

The first commercial catalyst for converting syngas to methanol was demonstrated by BASF in 1923 using ZnO-Cr_2O_3 catalyst which was only active at high temperature (350–400°C) and high pressure (240–350 bar) [44]. However, this catalyst easily poisoned with syngas containing impurities like sulfur, chlorine and heavy metals. Imperial Chemical Industry (ICI) introduced a more active and stable Cu/ZnO based catalyst in 1966 [39]. However, a careful analysis of literature data showed that the best systems for the hydrogenation of CO_2 to methanol are Cu/ZrO_2 based [50], although these are strongly influenced by operating conditions and the preparation methodology. In fact, in the step of catalyst design, in opposition to the traditional empirical approach, we need detailed knowledge of the required catalytic properties and particularly an adequate control of morphological properties (total surface area and metal surface structure, crystallinity); that is possible through a fine design of the catalytic system, adopting a suitable preparation method.

Although the Cu-based systems supported on ZnO are the most studied catalysts, nevertheless it is clear that the specific activity of copper does not seem apparently influenced by the nature of the carrier oxide. However, previous studies conducted by Chinchen et al. [51] showed that the Zn exerts many functions, giving the best performance among the different tested oxides (Cr_2O_3, SiO_2 and MnO). Zinc oxide acts as a geometrical spacer between Cu nanoparticles and thus plays a pivotal role in maintaining the active Cu metal in optimal dispersion in the Cu/ZnO catalyst, consequently providing a high number of active sites exposed to gaseous reactants [43]. Indeed, beyond to promote the increase of the surface area (especially with alumina), ZnO is enough refractory and it hinders the sintering of copper particles, acting like a dispersing agent of sulfur and chlorides as well, the main poisons for the catalyst. It also plays an important role to maintain an appropriate ratio Cu^+/Cu^0, since both states are involved in the synthesis, creating Cu^+-O-Zn type active sites and thus stabilizing the oxidation state of copper. Behrens *et al.* [42] have reported that ZnO can promote strong metal–support interaction with Cu species, which induces the formation of 'methanol-active copper'. Nakamura *et al.* [52] found that Zn shows a very good promoting effect in the synthesis of methanol, but not in rWGS reaction. Furthermore, addition of trivalent ions like Al^{3+} into the Cu/ZnO was found to improve stability along with Cu dispersion and metal surface area. Afterwards, a ternary Cu/ZnO/Al_2O_3 (CZA) catalyst started to be used for methanol synthesis operating at moderate pressure ranging from 50 to 100 bar and temperature of ca. 250 °C [37-42].

Although it is unanimously recognized the peculiar functionality both of copper and zinc oxide in the mechanism of CO_2 activation, for a further development of the catalytic system, the need for other metal oxides into the catalyst composition is also required, so to realize multimetallic systems more active than bimetallic catalysts in the formation of MeOH, which will be then dehydrated into DME. Really, many studies have already reported the unique features of various metals added in the catalyst composition as promoters of Cu-Zn based catalysts for the CO_2-to-MeOH hydrogenation reaction, like Al [53, 56], Mn [57, 58], Cr [59], Au [60], Zr [61-68], Pd [69-71], La [55, 72-73], Si [74, 75], Ce [55, 76], Ga [77, 78], V [79], carbon [80-82] or mixtures among them [55, 83-86] revealing a superior performance of Zr, Al and Ga in terms of activity, selectivity and stability.

4.2 Catalysts for MeOH-to-DME step

Dimethyl ether is produced via methanol dehydration step (MeOH-to-DME, MTD):

$$2CH_3OH = CH_3OCH_3 + H_2O$$

As discussed above, methanol dehydration is an exothermic reversible reaction that proceeds without mole number variation. For this reason, reaction pressure does not affect conversion equilibrium, while lower reaction temperatures have a thermodynamic benefit toward DME production. Methanol dehydration is an acid-catalyzed reaction and several investigations have been published with the aim to identify an active, selective and stable catalyst at relative low temperature for the above-mentioned thermodynamic advantages. Furthermore, for this technology there are several licensors including Haldor Tospoe, Linde/Lurgi, Toyo Engineering, Uhde, MGC (Mitsubishi Gas Chemical Company, China Southwestern Research Institute of Chemical Industry and China Energy (Jiutai Group)).

Depending on catalyst characteristics, methanol dehydration can be carried out in both vapour and liquid phase, with reaction temperature in the range 100-300 °C and pressure up to 20 bar. γ-Al_2O_3 is the most investigated catalyst for methanol dehydration. It is very attractive catalyst due its low cost, high surface area, high thermal and mechanical stability, and because it exhibits high selectivity toward DME also under extreme temperature (up to 400 °C) thanks to its weak Lewis acid sites that are not able to promote side reactions. Unfortunately, these acid characteristics require reaction temperature higher than 250-270°C to promote methanol conversion [85, 86] even if catalyst activity can be improved by modifying γ-Al_2O_3 surface with silica, phosphorous ($AlPO_4$), titanium, niobium, boron and others species [87-91].

Although γ-Al_2O_3 offers high selectivity towards DME, it tends to strongly adsorb the water produced during the reaction causing deactivation as demonstrated by several investigations [88, 92-95]. As described above, an important amount of water is produced especially in one-pot CO_2-to-DME process. Thus, γ-Al_2O_3, in spite of its several advantages, is not classified as a reliable catalyst for DME production by CO_2 hydrogenation as reported later.

Heteropoly acids (HPAs) can be also used to catalyze methanol dehydration reaction step. HPA-type materials can be represented by the formula $H_{8-n}[X_n^+M_{12}O_{40}]$, where X is the central atom (e.g. P^{5+}, Si^{4+}, Al^{3+}, etc.), n is its oxidation state and M is the metal ion. Because the high Brønsted acidity displayed from these materials, HPAs offer catalytic performances usually better than other solid catalysts such as zeolites, e.g. ZSM-5, especially at low temperature. Alharbi et al. [96] compared HPAs catalysts with ZSM-5 zeolites with different acidity (Si/Al=10-120). Results showed that tungsten/phosphorous-containing HPA (HPW) showed a turnover frequency (TOF) of about 53 h^{-1} while the most active ZSM-5 sample showed a TOF value of about 1 h^{-1}. The authors highlighted that the higher catalytic activity displayed by HPAs can be attributed to the higher acid sites strength of these materials. Furthermore, Ladera *et al.* [97] reported that the accessibility of methanol molecules to proton sites of HPAs can be improved by using TiO_2 as support.

Ion exchange resins (IERs) were also proposed as acid catalysts for methanol dehydration. Divinil benzene/styrene copolymers are usually used in which sulfonic acid groups are introduced being able to dehydrate methanol to DME. IERs have been considered attractive catalysts for MTD reaction because the high activity exhibited also at relatively low temperature (<150 °C) [98]. Recent works suggested Nafion resin, Nafion/silica composites or Amberlyst 35/36 as suitable catalysts for the synthesis of DME from methanol [99-101]. On the other hand, the application of ion exchange resins as acid catalyst in one-pot CO_2 hydrogenation to DME is hindered from the low thermal stability usually exhibited from these materials in the temperature range in which the process is usually performed (ca. 250 °C) [102].

4.2.1 Methanol dehydration over zeolites

Research is now focusing on use of zeolites as catalysts for methanol dehydration reaction step, especially, in view of a potential application as acid catalyst for one-pot CO_2-to-DME process. Zeolites are applied also in other catalytic processes concerning the reuse of carbon dioxide and production of alternative fuel such as dry reforming of methane [103-105] and biodiesel production by enzymatic catalysis [106, 107].

Zeolites are crystalline aluminosilicates whose catalytic properties are well-known for decades. The ever growing success of zeolites as catalysts in several industrial processes is mainly resulting from their unique molecular shape-selectivity due to a well-defined regular microporous structure. The possibility of tuning this system of voids (openings and spatial orientation of channels, size and location of cages, etc.) allows to have a catalyst that is able to catalyze the most desired reaction pathway. Beside shape-selectivity, the acid properties of zeolites are of paramount importance in catalysis. Generally, both Brønsted and Lewis type acid sites are simultaneously present in zeolites and their concentration, distribution, strength and location are well known factors affecting the overall activity, product selectivity and deactivation of the catalyst. This and more about the use of zeolites in catalysis is well described by Corma [108].

Several investigations were focused on use of ZSM-5 catalyst for methanol dehydration reaction, exhibiting, unlike γ-Al_2O_3, high resistance toward water adsorption as demonstrate by dedicated studies [85, 109]. Furthermore, due to its stronger acid sites (Lewis and/or Brønsted type), ZSM-5 offers high activity in terms of methanol conversion at relative low reaction temperature. For instance, Vishwanathan *et al.* [109] reported a value of methanol conversion of about 80% over H-ZSM-5 at 230°C, while over γ-Al_2O_3 conversion was just 5% and it is necessary to increase the temperature to 320 °C to reach 80%. Therefore, high activity of zeolites at relatively low temperature is important in terms of both process economy and thermodynamics as previously discussed. High activity is retained because ZSM-5 possesses medium and strong acid sites that allow a fast methanol conversion. Unfortunately, as mentioned above, strong acid sites of zeolites catalyze also side reactions involving methanol leading formation of by-products such as olefins and coke causing DME selectivity loss and deactivation.

The mechanism of DME formation over zeolites by methanol dehydration has been already investigated [110-113], demonstrating that DME formation mechanism involves formation of methoxyl ions by reaction between methanol and acid sites of catalyst, followed by combination of another alcohol molecule with methoxyl species to form the ether even if the associative mechanism involving two methanol molecules co-adsorbed on the same acid sites can not be excluded. On the contrary, in the temperature range of direct synthesis of DME (250–280°C), the strong acid sites of zeolite may convert the methanol into a wide range of hydrocarbons: from olefins (methanol–to–olefins process, MTO) [114,115] to aromatic species that are somehow linked to the olefins production, being involved in the (auto)–catalytic process known as "hydrocarbon pool" mechanism (HCP) [111,115-117]. Under the simultaneous presence of aromatic compounds, acid sites and high temperature, a favorable condition is realized for coke formation, a relevant aspect in MTO. Catalyst structure (channel size and configuration) is the most important factor addressing the pool-molecules formation. At high temperature, characteristic of MTO process, zeolite structures with large cages or 3–D channel system, as SAPO–34, BEA and MFI, promote the formation of aromatic compounds that can be entrapped in the structure or diffuse out. The most common aromatic species are in the class of poly–methylbenzenes, depending on the catalyst channel size: tri–methylbenzene is the most active species on MFI, while hexa–methylbenzene is the most active for olefins formation in the large cages of SAPO–34 and BEA [118]. These molecules are also considered as coke precursors and it is important to notice that they can be produced also in the lowest temperature range of MeOH–to–DME reaction. In these conditions these poly–methylbenzenes do not act as co-catalyst in HCP (because of the low temperature), accumulating in the structure as carbon deposits. Furthermore, in the case of either DME or olefins synthesis, it is well known that zeolite deactivation mainly comes from the coke deposition that causes pore blocking. In addition, it has been demonstrated that both catalyst structure and acidity strongly affect mechanism of coke formation in terms of composition, quantity and location. Campelo *et al.* [119] report a comparison between several silico–aluminophosphate with different channel configuration (1–, 2– and 3–dimensional) and it is showed that on a 3–dimensional structure (as SAPO–34), the oligomers formed in the channels can migrate to the big cages of this structure where react over strong acid sites leading to formation of heavier oligomers and aromatics that cannot back to the channels, so causing a rapid catalyst deactivation for pore blocking. On the other hand, deactivation of 1–dimensional large channels (as

SAPO–5) is due to the adsorption of multi–branched chains on the strong acid sites, also causing blocking of the pore system. Structures with both small/medium channels and cages, as MFI type, do not permit trapping of heavy compounds inside the crystal and coke is preferably formed on external surface of crystals, so that catalyst deactivation occurs by coke deposition on the mouth of the channels [120, 121]. Catalyst deactivation rate is also affected from crystal morphology: small or hierarchical crystals exhibit higher resistance to deactivation by coke deposition than large crystals with microporous texture [122, 123]. On small 1–D structures, as MTF, no hydrocarbon pool mechanism is observed even at high temperature (400°C) and DME is the only product detected in reactor out stream; nevertheless this structure exhibits fast deactivation over time [124] as consequence of carbon deposition. Therefore, catalyst structure may play a key role on product selectivity inhibiting either the hydrocarbon pool mechanism or the formation of coke precursors with the aim to increase the catalyst stability overtime.

Recently, several studies were dedicated to study the effect of zeolites structure on catalytic performances during methanol-to-DME reaction step at reaction temperature of direct synthesis (<280 °C).

On 2017, Catizzone *et al.* [125] studied methanol dehydration reaction on several zeolites (or molecular sieves) having different channel orientation (1-, 2- and 3-dimensional channel orientation) and channel openings (from 8- to 12-membered rings). Results clearly showed how the voids system of zeolites is of paramount importance for this reaction. 1-dimensional zeolites with large pore openings (e.g. MTW or MOR) show high selectivity towards DME (at 240 °C) but a fast deactivation was observed attributed to pore blocking by coke deposition. On the contrary, by using 1-dimensional zeolite with medium-pore openings (such as TON) both a higher stability towards deactivation and lower coke deposition was observed.

Zeolites with 3-dimensional channel orientation (e.g. MFI, BEA or SAPO-34 structure were also investigated by the authors [125, 126]. Despite the small channel openings of SAPO-34 (about 3.8 Å) conferring high selectivity towards DME, this catalyst is rapidly deactivated by coke formed and deposited into the large 3-dimensional channel intersection (about 7.4 Å large) that blocks reactant diffusion inside the crystal. On the contrary, when channel openings and intersections have similar size (e.g in the case of BEA or MFI structure) a higher stability was observed even if by-products (e.g. C2-C6 olefins) were detected in reaction out-stream and a high coke deposition rate was observed [127].

Coke deposited during methanol dehydration to DME over zeolites mainly consists of poly-methylbenzenes (PMB, from xylenes to hexa-methyl benzene) with a grade of substitution function of the channel system. For instance, the 1-D medium pore channel system of TON inhibits the formation PMB heavier than tri-methyl benzene; on the contrary, despite the similar channel openings of TON, EUO-type structure accommodates also hexa-methyl benzene due to the presence side-pockets large enough to permit the formation of this molecule. Zeolites with large pore system such as beta, also allows deposition of polycyclic species while carbon phase deposited of FER-type crystals selectively consists of tetra-methyl benzene compound probably located in ferrierite cages [125].

Coke formation can be reduced by post-synthesis treatment or by a careful tailoring of the textural properties. A dual pore size distribution (e.g. micro- and meso-pores) is a reliable configuration to reduce coke formation and postpone catalyst deactivation during methanol dehydration. Tang *et al.* [128] reported that a ZSM-5/MCM-41 composite material with both microporous and mesoporous allows to obtain higher activity and higher stability compared with ZSM-5 with only microporous structure. Similar results were obtained by Rutkowska *et al.* [129] which show that hierarchical ZSM-5 material (interconnected micro/meso-pores) exhibit a lower coke formation rate than microporous ZSM-5.

On the whole, several results suggest FER zeolite as a reliable catalyst to selectively transform methanol to DME [125, 130, 131]. Thanks to its 8-/10-membered ring 2-dimensional channel system, FER structure shows a high DME selectivity, a slow coke deposition and a high resistance to deactivate.

Beside structure, also acidity properties of zeolites strongly affect catalytic behaviour of these materials. High catalytic performances in terms of DME selectivity were obtained by decreasing acid sites strength by modifying zeolite surface [132-133] or by decreasing total acidity [109, 134, 135].

Kim *et al.* [132] studied methanol dehydration reaction over ZSM-5 zeolites impregnated with different γ-Al_2O_3 loading and compared the catalysts in terms of operative temperature range (OTR) defined as the temperature range giving methanol conversion higher than 50% and DME selectivity higher than 99%. The authors found that OTR of 210-310 °C and 320-370 °C were evaluated for bare ZSM-5 and γ-Al_2O_3 confirming that zeolite is more active but less selective than γ-Al_2O_3. On the contrary, a hybrid catalyst γ-Al_2O_3/ZSM-5 containing 70% γ-Al_2O_3 exhibited a OTR of 230-380°C showing, therefore, higher activity than γ-Al_2O_3 but also higher selectivity than both γ-Al_2O_3 and bare ZSM-5 thanks to the adequate dilution of strong acid sites of zeolite after impregnation.

Similar results were obtained by other authors by impregnation of ZSM-5 catalyst with sodium, magnesium, zinc or zirconium [133, 134]. The authors showed that metal loading decreases strong acidity and increases weak acidity obtaining a catalyst less active towards hydrocarbon formation. For instance, Khandan *et al.* [134] reported that, DME yield increased from 53% to 93% after impregnation of ZSM-5 with zirconium; moreover, stability tests showed that resistance towards deactivation was also improved.

Acidity in zeolites can be also decreased by reducing the aluminum content or increasing the Si/Al ratio [135, 136]. In this concern, Hassanpour *et al.* [135] prepared ZSM-5 catalysts in a wide range of Si/Al ratio (Si/Al=25-250) and tested them in methanol conversion at 300 °C. The authors found that by-products formation (e.g. ethylene, propylene) decreases as the Si/Al increases obtaining higher DME selectivity for catalysts with lower total acidity.

Catizzone *et al.* [131] have recently reported some aspects concerning the role of acid sites of FER-type zeolites by preparing catalysts with different Si/Al ratio. The authors reported that higher methanol conversion level can be achieved over FER zeolites with higher aluminum content but, experimental evidences also demonstrated that lattice Lewis acid sites are more active than Brønsted sites even if a reaction temperature lower than 260-280 °C should be adopted in order to prevent by-products formation (especially methane). As previously discussed about thermodynamic aspects, a good catalyst for methanol dehydration step should promote high methanol conversion at temperature lower than 240-260 °C. The superiority of FER zeolite over γ-Al_2O_3 and several other zeolites at temperature lower than 240 °C was recently [125]. In this paper, the authors showed that, at only 200 °C, methanol conversion was about 82% over FER with a 100% of DME selectivity while a methanol conversion level of 25% only was observed for commercial γ-Al_2O_3. As will be discussed below, recent studies consider FER-type zeolite as a good acid function for preparing an attractive hybrid catalyst for CO_2 hydrogenation to DME.

4.3 Catalysts for one-pot CO_2 hydrogenation to DME

The catalyst for the direct CO_2-to-DME conversion should be able to efficiently catalyze both reaction methanol synthesis and its dehydration, minimizing the yield of CO formed by the Reverse Water Gas Shift (rWGS) side reaction and hydrocarbons involving in methanol conversion. A huge amount of water formed during CO2 hydrogenation to DME thermodynamically limits both formation and dehydration of methanol causing DME yield lower than that obtained via CO hydrogenation [85].

In this concern, the acid catalyst must be stable in presence of water and the acid sites must be well distributed and not to strong in order to inhibit hydrocarbons formation [85, 89, 137-144]. In this sense, as described above, zeolites seem to offer the highest versatility in terms of higher number of acid sites, water resistance and shape-selectivity toward desired compound. A list of some results [77, 145-157] concerning one-pot CO_2 hydrogenation to DME is reported in Table 4.

The first studies on hybrid/bifunctional catalytic systems active in the direct hydrogenation reaction of CO_2 involved the use of physical mixtures between the methanol synthesis catalyst (MSC) and an acid system, typically a Cu-ZnO-Al_2O_3 system for the synthesis of MeOH and γ-Al_2O_3 or zeolites as acid solids for the dehydration of MeOH (see Paragraph 4.2).

665 **Table 4.** Recent investigated catalysts for one-pot CO_2-to-DME process. PM: physical mixing; WM: wet
666 mixing; CP: co-precipitation; IM: impregnation; GHSV: Gas Hourly Space Velocity; P: reaction pressure;
667 T: reaction temperature; X_{CO2}: conversion of CO_2; Y_i: carbon-basis yield of *i*-product.

Catalyst	Preparation Method	H_2/CO_2	GHSV ($NmL \cdot g^{-1} \cdot h^{-1}$)	P;T (MPa;°C)	X_{CO2} (%)	Y_{CO} (%)	Y_{MeOH} (%)	Y_{DME} (%)	Ref.
Cu/Zn/Al HZSM5	PM	3	3000	5;260	31	2	9.3	19	[145]
Cu/Zn/Al γ-Al2O3					20	11.6	8	0.4	
Cu/Zn/Al/Zr ZSM5	WM	3	3100	3;260	24.1	7	10.6	6.4	[146]
Cu/Zn/Zr Ga-Sil1	CP	3	1200	3;250	19.0	6.4	4	8.6	[147]
Cu/Ti/Zr ZSM5	WM	3	1500	3;250	15.6	6.1	2.0	7.4	[148]
Cu/Zn/Zr/V ZSM5	CP	3	1500	3;270	32.5	9.1	4.3	19.1	[77]
Cu/Zn/Al/Zr ZSM5	PM	3	6000	5;270	27.5	-	5.0	16	[149]
Cu/Zn/Al/La ZSM5	PM	3	3000	3;250	43.8	0.11	1.9	31.2	[150]
Cu/Mo ZSM5	IM	2	1500	3;240	12.4	2	0.7	9.5	[151]
Cu/Zn/Zr/Pd ZSM5	CP	3	1800	3;200	18.7	2.4	2.5	13.8	[152]
Cu/Zn/Al ZSM5+CNTs	PM	3	1800	3;260	46.2	8.9	16.4	21	[153]
Cu/Zn/Zr FER	CP	3	8800	5;260	23.6	9.2	3.5	10.6	[154]
Cu/Zn/Al ZSM5	CP	3	750	4;275	35	-	-	23	[155]
Cu/Zn/Al γ-Al2O3					40			10	
Cu/Zn/Al Amorphous silica-alumina	CP	3	1800	3;270	47.1	12.3	14.7	20.1	[156]
Cu/Fe/Zr ZSM5	PM	5	1500	3;260	28.4	2.2	4.2	18.3	[157]

668
669 Zeolites, in particular, have shown greater efficiency than γ-Al_2O_3 as an acid component of the
670 bifunctional catalyst, considering that ability to modulate acidity (in terms of number, type and

strength of acid sites) enables direct synthesis of DME at low temperatures, where the formation of methanol is thermodynamically favored. For instance, Naik *et al.* [145] compared catalytic activity of hybrid catalysts prepared by mechanical mixing of MSC and γ-Al_2O_3 or ZSM-5 (Si/Al=60). Catalytic tests carried out in a fixed-bed reactor at 260 °C and 5 MPa, revealed that MSC/ZSM-5 exhibits a superior catalytic behavior than MSC/ γ-Al_2O_3in terms of CO_2 conversion (ca. 30% vs. ca. 20%), DME selectivity (ca. 75% vs. ca. 5%) and stability. As a conclusion, DME yield was about 20% over MSC/ZSM-5 and lower than 1% over MSC/ γ-Al_2O_3suggesting that γ-Al_2O_3 can not be considered as a valuable acid catalyst for one-pot CO_2-to-DME process.

Compared to the conventional mechanical mixing between a methanol synthesis catalyst and a zeolite, the generation of metal oxide and acid sites in a single system is capable of improving the conversion of CO_2, enabling even higher rates of formation/dehydration of methanol on the neighboring surface sites. Different strategies have been applied to prepare the bifunctional catalysts for direct DME synthesis. For instance, methods comprising impregnation, co-precipitation [158-162] or sol–gel steps (or their combinations) [44, 163] and even more sophisticated approaches leading to core–shell catalyst structures [164-166] have been reported. Nevertheless, there are different opinions on the efficiency of bifunctional catalysts in comparison to admixed systems. Sun et al. prepared bifunctional catalysts by co-precipitation sedimentation of a ZrO_2-doped CZA-component on an H-ZSM5 zeolite [152, 167].

According to them, bifunctional catalysts lead to high CO-conversions because the two types of active sites are in close contact with each other. This enables the generation of DME directly from an adsorbed methoxy-species without the intermediary synthesis of methanol.

Ge *et al.* also concluded that both active sites need to be in close contact so that a synergistic effect can be achieved, which leads to higher catalytic activity [44]. However, Ge *et al.* stressed that coverage of both active sites during catalyst synthesis needs to be avoided.

A coverage of the active sites leads to a drop in activity due to the synthesis of inactive species and due to a decrease in active surface area. García-Trenco *et al.* stated that admixed catalyst systems are superior to bifunctional systems [168]. According to them, the preparation procedure of bifunctional catalysts can lead to a decrease of surface area due to a blockage of pores. However, they also stated that further interactions between the two active components, which have not been elucidated yet, influence catalyst activity as well.

Although the design of the catalytic system ideal for the hydrogenation of CO_2 does not require properties such as selectivity of shape and/or size, due to the small size of the molecules involved, the zeolites still have a high potential expressed through multiple properties such as the ability to modulate acidity, high surface area, microporosity or supporting properties, which represent the fundamental reasons why these unique structures are used as metal and / or metal oxide carriers in most of current catalytic systems.

Frusteri *et al.* [161] have recently investigated the role of acid sites of hybrid catalysts prepared via gel-oxalate precipitation of CuZnZr precursors of ZSM-5 crystals with a Si/Al ratio in the range 27-127. Results displayed that acidity of zeolite must be carefully tuned aiming to achieve a compromise between catalytic activity and resistance to deactivation by water. In particular, ZSM-5 with high Si/Al ratio (e.g. 127) showed high resistance in presence of water but low capacity to dehydrate methanol, while more acidic samples (e.g. ZSM-5 with Si/Al ratio of 27) offers high methanol conversion but poor water resistance and low DME selectivity; the author found that, for ZSM-5 zeolite, a Si/Al ratio of 38 showed the best performances in terms of CO_2 conversion, DME yield and water resistance.

Beside acidity, also textural properties of zeolite crystals strongly affect catalytic behavior of hybrid catalyst. In this concern, Frusteri *et al.* [158] have recently studied one-pot CO_2-to-DME reaction over hybrid grain prepared via co-precipitation of CuZnZr precursors over zeolite crystals with different channel system (i.e. MOR, FER and MFI). The microscopy analysis of hybrid grains highlighted that zeolite crystal features strongly affect metal oxides distribution obtaining a more homogenous distribution over lamellar FER-type crystals while formation of metal clusters on the other zeolite crystals. Catalytic results revealed that DME productivity followed the order

CuZnZr/FER>CuZnZr/MOR>CuZnZr/MFI. The authors related the superior catalytic activity of FER-based catalyst to the lower mass transfer limitations between metal/oxides(s) offered by anchorage of metal-oxide clusters on the lamellar crystals typical of FER zeolite as well as to the larger population of Lewis basic sites generated of FER surface able to activate carbon dioxide promoting its conversion. Nevertheless, an important deactivation of the catalyst was observed during time-on-stream tests.

The hybrid catalysts up to now developed are generally prone to deactivation caused by either coke deposition or metal sintering or poisoning from contaminants present in the reaction stream leading to the blockage of active sites [169, 170]. As mentioned before, for hydrocarbon reactions over zeolites, deactivation is mainly attributed to two main mechanisms: 1) the acid site coverage which deactivates the catalyst by coke adsorption; 2) pore blockage due to deposition of carbonaceous compounds in cavities or channel intersections that makes pores inaccessible [171]. In addition, it is well known that coke formation on zeolites is a shape-selective process. Under comparable conditions, large-pore zeolites are more susceptible to deactivation by coke deposition than medium-pore zeolites [172]. Although H-ZSM-5 is not sensitive to water [173, 174], it shows high activity for the transformation of DME into hydrocarbon byproducts. These hydrocarbons can further evolve into heavy structures (coke) and consequently can block the zeolite pores and cause its deactivation, as previously discussed. However, this deactivation is slow due to the high partial pressure of hydrogen that attenuates the mechanism of coke formation [148]. This phenomenon can be controlled by employing a suitable concentration of Na in zeolite in order to moderate the number of Brønsted sites and to reduce the acid strength of the H-ZSM-5 zeolite [170]. The addition of Silicalite-1 shell to the ZSM-5 zeolite is also considered as an efficient method for improving the resistance toward carbon formation [174]. Also reactor configuration strongly affects catalyst deactivation: considering that the reactors mostly used in the production of DME are slurry reactors and fixed bed reactors, the bifunctional catalysts were seen to deactivate more quickly in the slurry reactor than in the fixed-bed reactor [175].

These examples show that a deeper understanding of the underlying mechanisms and interactions between the two active components in admixed as well as bifunctional catalysts is necessary. Furthermore, the influence of catalyst composition and features on catalytic activity and stability should be studied more in detail so that a comparison of catalysts independent of the respective preparation method will be possible.

5. Conclusions and perspectives on the catalyst development

Zeolites are unique materials with huge catalytic potential in several industrial processes, recently determining a huge research interest as dehydration components in the DME synthesis, started not only from methanol but even from CO_2-rich streams recycled for hydrogenation. From the analysis of the thermodynamic equilibriums involved in the hydrogenation of CO_2, it has been demonstrated that the production of DME is favored at high pressure and low temperature for achieving both high conversion and DME yield. During CO_2-to-DME hydrogenation reaction ($P \geq 30$ bar MPa; $T \leq 260$°C) the use of zeolites does not imply to simply exploit their typical shape/size selectivity, but other important features are involved, such as tunable solid acidity, high surface area, microporosity or loading property, representing the fundamental reasons why these unique structures are utilized as carriers of metals and/or metal-oxides.

Generally, a mechanical mixture of mixed oxides (containing Cu as active species for the synthesis of methanol) and a zeolite, typically ZSM-5, have been mainly proposed as an effective catalytic system. However, recent papers claimed alternative zeolite structures as more suitable in the process, evidencing as the zeolite topology significantly affects the physicochemical properties of the catalysts as well as the catalytic performance. In particular, some fundamental aspects have been indicated as crucial for high process productivity: i) the zeolite must be stable in presence of water; ii) the formation of olefins should be inhibited; iii) the acid sites must be well distributed and of suitable strength. Moreover, the performance of multi-site systems for the direct conversion of CO_2 into DME has been also proved, so demonstrating the possibility to integrate the two methanol-

775 synthesis and methanol-dehydration functionalities at level of single grain during preparation. Apart
776 from the need of optimal experimental parameters, the crucial issue for preparing a high-active
777 hybrid catalyst is optimizing the formulation and interaction of the different metallic, oxide(s) and
778 acidic components, so to realize a punctual mix of surface sites necessary for the primary formation
779 of methanol, followed by its dehydration to DME on acid sites of the zeolite. Overall, in the
780 perspective to develop an active and stable multi-site catalyst for the production of DME from CO_2,
781 the concurrence of textural, structural and surface factors must be adequately balanced.
782

Acknowledgments: Part of this work was realized within the bilateral agreement of Scientific and Technological Cooperation CNR-MTA/HAS (Hungarian Academy of Sciences).

Conflicts of Interest: The authors declare no conflict of interest.

References

1. Zhou, P.; Wang, M. Carbon dioxide emissions allocation: a review. *Ecol. Econ* **2016**, *125*, 47-59, DOI: 10.1016/j.ecolecon.2016.03.001
2. de Conik, H.; Benson, S.M. Carbon dioxide capture and storage: issues and prospects. *Annu. Rev. Environ. Resour.* **2014**, *39*, 243–270, DOI: 10.1146/annurev-environ-032112-095222
3. Olah, G.A. Beyond oil and gas: the methanol economy. *Angew. Chem. Int. Ed.* **2005**, *44*, 2636–2639, DOI: 10.1002/anie.200462121
4. Tian, P.; Wei Y.; Ye M.; Liu Z. Methanol to olefins (MTO): from fundamentals to commercialization *ACS Catal.* **2015**, *5*, 1922–1938, DOI: 10.1021/acscatal.5b00007
5. Keil F.J. Methanol-to-hydrocarbons: process technology. *Microp. Mesopor. Mater.* **1999**, *29*, 49–66, DOI: 10.1016/S1387-1811(98)00320-5
6. Arcoumanis C.; Bae C.; Crookes R.; Kinoshita E. The potential of di-methyl ether (DME) as an alternative fuel for compression-ignition engines: A review. *Fuel* **2008**, *87*, 1014–1030, DOI: 10.1016/j.fuel.2007.06.007
7. Ogawa T.; Inoue N.; Shikada T.; Ohno Y. Direct dimethyl ether synthesis. *J. Nat. Gas Chem.* **2003**, *12*, 219–227.
8. Cheng C.; Zhang H.; Ying W.; Fang D. Intrinsic kinetics of one-step dimethyl ether synthesis from hydrogen-rich synthesis gas over bi-functional catalyst. *Korean J. Chem. Eng.* **2011**, *28*, 1511–1517, DOI: 10.1007/s11814-011-0018-4
9. Trippe. F.; Frohling, M.; Schultmann, F.; Stahl, R.; Henrich, E.; Dalai, A.; Trippe, Frederik, et al. "Comprehensive techno-economic assessment of dimethyl ether (DME) synthesis and Fischer–Tropsch synthesis as alternative process steps within biomass-to-liquid production. *Fuel Process. Technol.* **2013**, *106* 577-586, DOI: 10.1016/j.fuproc.2012.09.029
10. US Patent 5, 632, 786, May 27, 1997, A. Basu et al. (Eds.).
11. Centi G.; Quadrelli E.A.; Perathoner S. Catalysis for CO 2 conversion: a key technology for rapid introduction of renewable energy in the value chain of chemical industries. *Energy Environ. Sci.* **2013**, *6*, 1711–1731, DOI: 10.1039/C3EE00056G.
12. Tamagnini P.; Axelsson R.; Lindberg P.; Oxelfelt F.; Wunschiers R.; Lindblad P. Renewable hydrogen production. *Microbiol. Mol. Biol. Rev.* **2006**, *66*, 1–20, DOI: 10.1002/er.1372
13. Chaubey R.; Sahu S.; James O.O.; Maity S. A review on development of industrial processes and emerging techniques for production of hydrogen from renewable and sustainable sources. *Renew. Sustain. Energy Rev.* **2013**, *23* 443–462, DOI: 10.1016/j.rser.2013.02.019
14. Parthasarathy P.; Narayanan K.S. Hydrogen production from steam gasification of biomass: influence of process parameters on hydrogen yield–a review. *Renew. Energy* **2014**, *66*, 570–579, DOI: 10.1016/j.renene.2013.12.025
15. Kalinci Y.; Hepbasli A.; Dincer I. Biomass-based hydrogen production: a review and analysis. *Int. J. Hydrogen Energy* **2009**, *34*, 8799–8817, DOI: 10.1016/j.ijhydene.2009.08.078
16. Ni M.; Leung M.K.H.; Leung D.Y.C.; Sumathy K. A review and recent developments in photocatalytic water-splitting using TiO2 for hydrogen production. *Renew. Sustain. Energy Rev.* **2007**, *11*, 401–425, DOI: 10.1016/j.rser.2005.01.009
17. Ismail A.A.; Bahnemann D.W. Photochemical splitting of water for hydrogen production by photocatalysis: a review. *Sol. Energy Mater. Sol. Cells* **2014**, *128* 85–101, DOI: 10.1016/j.solmat.2014.04.037
18. Álvarez A.; Bansode A.; Urakawa A.; Bavykina A.V.; Wezendonk T.A.; Makkee M.; Gascon J.; Kapteijn F. Challenges in the Greener Production of Formates/Formic Acid, Methanol, and DME by Heterogeneously Catalyzed CO2 Hydrogenation Processes. *Chem. Rev.* **2017**, 117, 9804–9838, DOI: 10.1021/acs.chemrev.6b00816
19. Semelsberger T.A.; Borup R.L.; Greene H.L. Dimethyl ether (DME) as an alternative fuel. *J. Power Sources* **2006**, *156*, 497–511, DOI: 10.1016/j.jpowsour.2005.05.082

20. Park S.H.; Lee C.S. Combustion performance and emission reduction characteristics of automotive DME engine system. *Prog. Energy Combust. Sci.* **2013**, *39*, 147–168.
21. Sidhu S.; Graham J.; Striebich R. Semi-volatile and particulate emissions from the combustion of alternative diesel fuels. *Chemosphere* **2001**, *42*, 681–690, DOI: 10.1016/S0045-6535(00)00242-3
22. Kim M.Y.; Yoon S.H.; Ryu B.W.; Lee C.S. Combustion and emission characteristics of DME as an alternative fuel for compression ignition engines with a high pressure injection system. *Fuel* **2008**, *87*, 2779–2786, DOI: 10.1016/j.fuel.2008.01.032
23. Egnell R.; SAE Tech. Pap. 2001. SAE 2001-01-0651 (2001).
24. Teng H.; McCandless J.C.; Schneyer J.B. SAE Tech. Pap. 2001. SAE 2001-01-0154 (2001).
25. Fleisch T.H.; Basu A.; Gradassi M.J.; Massin J.G. Dimethyl ether: a fuel for the 21st century." *studies in surface science and catalysis Stud. Surf. Sci. Catal.* **1997**, *107*, 117-125, DOI: 10.1016/S0167-2991(97)80323-0
26. Gupta K.K.; Rehman, A.; Sarviya, R.M. Bio-fuels for the gas turbine: A review. *Renew. Sustain. Energy Rev.* **2010** *14* 2946–2955, DOI: 10.1016/j.rser.2010.07.025
27. Lee M.C.; Seo S.B.; Chung J.H.; Joo, Y.J.; Ahn, D.H. Combustion performance test of a new fuel DME to adapt to a gas turbine for power generation. *Fuel* **2008**, *87*, 2162 – 2167, DOI: 10.1016/j.fuel.2007.11.017
28. Lee, M.C.; Seo, S.B.; Chung, J.H.; Joo, Y.J.; Ahn, D.H. Industrial gas turbine combustion performance test of DME to use as an alternative fuel for power generation. *Fuel* **2009**, *88*, 657–662, DOI: 10.1016/j.fuel.2008.10.027
29. Lee, M.C.; Yoon, Y. Development of a gas turbine fuel nozzle for DME and a design method thereof. *Fuel* **2012**, *102*, 823–830, DOI: 10.1016/j.fuel.2012.05.017
30. Haryanto, A.; Fernando, S.; Murali, N.; Adhikari, S. Current status of hydrogen production techniques by steam reforming of ethanol: a review. *Energy Fuels* **2005**, *19*, 2098–2106, DOI: 10.1021/ef0500538
31. Ghenciu, A.F. Review of fuel processing catalysts for hydrogen production in PEM fuel cell systems. *Curr. Opin. Solid State Mater. Sci.* **2002**, *6*, 389–399, DOI: 10.1016/S1359-0286(02)00108-0
32. Palo, D.R.; Dagle, R.A.; Holladay J. D. Methanol steam reforming for hydrogen production. *Chem. Rev.* **2007**, *107*, 3992–4021, DOI: 10.1021/cr050198b
33. Takeishi, K.; Suzuki, H. Steam reforming of dimethyl ether. *Appl. Catal. A* **2004**, *260*, 111–117, DOI: 10.1016/j.apcata.2003.10.006
34. Vicente, J.; Gayubo, A.G.; Ereña, J.; Aguayo, A.T.; Olazar, M.; Bilbao, J. Improving the DME steam reforming catalyst by alkaline treatment of the HZSM-5 zeolite. *Appl. Catal. B* **2013**, *130-131*, 73–83, DOI: 10.1016/j.apcatb.2012.10.019
35. Gazsi, A.; Ugrai, I.; Solymosy, F. Production of hydrogen from dimethyl ether on supported Au catalysts. *Appl. Catal. A* **2011**, *391*, 360–366, DOI: 10.1016/j.apcata.2010.04.054
36. Semelsberger, T.A.; Ott, K.C.; Borup, R.L.;. Greene, H.L. Generating hydrogen-rich fuel-cell feeds from dimethyl ether (DME) using physical mixtures of a commercial Cu/Zn/Al 2 O 3 catalyst and several solid–acid catalysts. *Appl. Catal. B* **2006**, *65*, 291–300, DOI: 10.1016/j.apcatb.2006.02.015
37. Jeong, J.W.; Ahn, C.-I.; Lee, D.H.; Um, S.H.; Bae, J.W. Effects of Cu–ZnO Content on Reaction Rate for Direct Synthesis of DME from Syngas with Bifunctional Cu–ZnO/γ-Al2O3 Catalyst.*Catal. Lett.* **2013**, *143*, 666–672, DOI: 10.1007/s10562-013-1022-6
38. Asthana, S.; Samanta, C.; Bhaumik, A.; Banerjee, B.; Voolapalli, R.K.; Saha, B. Direct synthesis of dimethyl ether from syngas over Cu-based catalysts: Enhanced selectivity in the presence of MgO. *J. Catal.* **2016**, *334*, 89–101, DOI: 10.1016/j.jcat.2015.10.020
39. Wender, I. Reactions of synthesis gas. *Fuel Process. Technol.* **1996**, *48*, 189–297, DOI: 10.1016/S0378-3820(96)01048-X
40. Huang, M.H.; Lee, H.M.; Liang, K.C.; Tzeng, C.C.; Chen, W.H. An experimental study on single-step dimethyl ether (DME) synthesis from hydrogen and carbon monoxide under various catalysts *Int. J. Hydrogen Energy* **2015**, *40*, 13583–13593, DOI: 10.1016/j.ijhydene.2015.07.168
41. Sousa-Aguiar, E.F.; Appel, L.G.; Mota, C. Natural gas chemical transformations: The path to refining in the future. *Catal. Today* **2005**, *101*, 3–7, DOI: 10.1016/j.cattod.2004.12.003
42. Bae, J.W.; Potdar, H.S.; Kang, S.-H.; Jun, K.-W. Coproduction of methanol and dimethyl ether from biomass-derived syngas on a Cu− ZnO− Al2O3/γ-Al2O3 hybrid catalyst. *Energy Fuels* **2008**, *22*, 223–230, DOI: 10.1021/ef700461j.

43. Aguayo, A.T.; Ereña, J.; Mier, D.; Arandes, J.M.; Olazar, M.; Bilbao J. Kinetic Modeling of Dimethyl Ether Synthesis in a Single Step on a CuO− ZnO− Al2O3/γ-Al2O3 Catalyst. *Ind. Eng. Chem. Res.* **2007**, *46*, 5522–5530, DOI: 10.1021/ie070269s
44. Ge, Q.; Huang, Y.; Qiu, F.; Li, S. Bifunctional catalysts for conversion of synthesis gas to dimethyl ether. *Appl. Catal. A* **1998**, *167*, 23–30, DOI: 10.1016/S0926-860X(97)00290-1
45. Wang, Z.; Wang, J.; Diao, J.; Jin, Y. The synergy effect of process coupling for dimethyl ether synthesis in slurry reactors. *Chem. Eng. Technol.* **2001**, *24*, 507–511.
46. Fleisch T.H.,. Basu A, Sills R.A. Introduction and advancement of a new clean global fuel: The status of DME developments in China and beyond. *J. Nat. Gas Sci. Eng.* **2012**, *9*, 94–107, DOI: 10.1016/j.jngse.2012.05.012
47. Wambach, J.; Baiker, A.; Wokaum, A. CO 2 hydrogenation over metal/zirconia catalysts. *Phys. Chem. Chem. Phys.* **1999**, *1*, 5071-5080, DOI: 10.1039/A904923A
48. Sugawa, S.; Sayama, K.; Arakawa, H. Methanol synthesis from CO 2 and H 2 over silver catalyst. *Energy Convers. Manage.* **1995**, *36*, 665-668, DOI: 10.1016/0196-8904(95)00093-S
49. Centi, G.; Perathoner, S. Advances in Catalysts and Processes for Methanol Synthesis from CO_2. In *CO_2: A Valuable Source of Carbon* Springer-Verlag, London, 2013; pp. 147–169.
50. Koppel, R.A.; Stocker, C.; Baiker, A. Copper-and silver–zirconia aerogels: preparation, structural properties and catalytic behavior in methanol synthesis from carbon dioxide. *J. Catal.* **1998**, *179*, 515-527, DOI: 10.1006/jcat.1998.2252
51. Chinchen, G.C.; Mansfield, K.; Spencer, M.S. The methanol synthesis-how does it work. *Chemtech* **1990**, *11*, 692.
52. Nakamura, J.; Nakamura, I.; Uchijima, T.; Kanai, Y.; Watanabe, T. Methanol synthesis over a Zn-deposited copper model catalyst. *Catal. Lett.* **1995**, *31*, 325.
53. Wang, X.; Zhang, H.; Li, W. In situ IR studies on the mechanism of methanol synthesis from CO/H 2 and CO 2/H 2 over Cu-ZnO-Al 2 O 3 catalyst. *Korean J. Chem. Eng.* **2010**, *27*, 1093–1098, DOI: 10.1007/s11814-010-0176-9.
54. Samei, E.; Taghizadeh, M.; Bahmani, M. Enhancement of stability and activity of Cu/ZnO/Al 2 O 3 catalysts by colloidal silica and metal oxides additives for methanol synthesis from a CO 2-rich feed. *Fuel Process. Technol.* **2012**, *96*, 128–133, DOI: 10.1016/j.fuproc.2011.12.028
55. Gao, P.; Li, F.; Zhao, N.; Xiao, F.; Wei, W.; Zhong, L.; Sun, Y. Influence of modifier (Mn, La, Ce, Zr and Y) on the performance of Cu/Zn/Al catalysts via hydrotalcite-like precursors for CO 2 hydrogenation to methanol. *Appl. Catal. A* **2013**, *468*, 442-452, DOI: 10.1016/j.apcata.2013.09.026
56. Słoczyński, J.; Grabowski, R.; Kozłowska, A.; Olszewski, P.; Lachowska, M.; Skrzypek, J.; Stoch, J. Effect of Mg and Mn oxide additions on structural and adsorptive properties of Cu/ZnO/ZrO 2 catalysts for the methanol synthesis from CO 2. *Appl. Catal. A* **2003**, *249*, 129–138, DOI: 10.1016/S0926-860X(03)00191-1
57. Fujiwara, M.; Ando, H.; Tanaka, M.; Souma, Y. Hydrogenation of carbon dioxide over Cu–Zn–Cr oxide catalysts. *Bull. Chem. Soc. Jpn.* **1994**, *67*, 546-550, DOI: 10.1246/bcsj.67.546
58. Pasupulety, N.; Driss, H.; Alhamed, Y.A.; Alzahrani, A.A.; Daous, M.A.; Petrova, L. Studies on Au/Cu–Zn–Al catalyst for methanol synthesis from CO 2. *Appl. Catal. A* **2015** *504* 308–318, DOI: 10.1016/j.apcata.2015.01.036
59. Arena, F.; Barbera, K.; Italiano, G.; Bonura, G.; Spadaro, L.; Frusteri, F. Synthesis, characterization and activity pattern of Cu–ZnO/ZrO 2 catalysts in the hydrogenation of carbon dioxide to methanol. *J. Catal.* **2007** *249* 185–194, DOI: 10.1016/j.jcat.2007.04.003
60. Arena, F.; Italiano, G.; Barbera, K.; Bordiga, S., Bonura, G.; Spadaro, L.; Frusteri, F. Solid-state interactions, adsorption sites and functionality of Cu-ZnO/ZrO 2 catalysts in the CO 2 hydrogenation to CH 3 OH. *Appl. Catal. A* **2008**, *350*, 16–23, DOI: 10.1016/j.apcata.2008.07.028
61. Bonura, G.; Cordaro, M.; Cannilla, C.; Arena, F.; Frusteri F. The changing nature of the active site of Cu-Zn-Zr catalysts for the CO 2 hydrogenation reaction to methanol. *Appl. Catal. B* **2014**, *152–153*, 152–161, DOI: 10.1016/j.apcatb.2014.01.035
62. Guo, X.; Mao, D.; Lu, G.; Wang, S.; Wu, G. Glycine–nitrate combustion synthesis of CuO–ZnO–ZrO 2 catalysts for methanol synthesis from CO 2 hydrogenation. *J. Catal.* **2010**, *271*, 178–185, DOI: 10.1016/j.jcat.2010.01.009

63. Donphai, W.; Piriyawate, N.; Witoon, T.; Jantaratana, P.; Varabuntoonvit, V.; Chareonpanich, M. Effect of magnetic field on CO 2 conversion over Cu-ZnO/ZrO 2 catalyst in hydrogenation reaction. *J. CO2 Util.* **2016**, *16*, 204–211, DOI: 10.1016/j.jcou.2016.07.007
64. Arena, F.; Italiano, G.; Barbera, K.; Bonura, G.; Spadaro, L.; Frusteri F. Basic evidences for methanol-synthesis catalyst design. *Catal. Today* **2009**, *143*, 80–85, DOI: 10.1016/j.cattod.2008.11.022
65. Gao, P.; Li, F.; Zhan, H.; Zhao, N.; Xiao, F.; Wei, W.; Zhong, L.; Wang, H.; Sun, Y. Influence of Zr on the performance of Cu/Zn/Al/Zr catalysts via hydrotalcite-like precursors for CO 2 hydrogenation to methanol. *J. Catal.* **2013**, *298*, 51–60, DOI: 10.1016/j.jcat.2012.10.030
66. Yang, C.; Ma, Z.Y.; Zhao, N.; Wei, W.; Hu, T.D.; Sun, Y.H. Methanol synthesis from CO 2-rich syngas over a ZrO2 doped CuZnO catalyst. *Catal. Today* **2006**, *115*, 222–227, DOI: 10.1016/j.cattod.2006.02.077
67. Melián-Cabrera, I.; Granados L.; Fierro, J.L.G. Pd-modified Cu–Zn catalysts for methanol synthesis from CO 2/H 2 mixtures: catalytic structures and performance. *J. Catal.* **2002**, *210*, 285–294, DOI: doi.org/10.1006/jcat.2002.3677
68. Sahibzada, M. Pd-promoted Cu/ZnO catalyst systems for methanol synthesis from CO2/H2. *Chem. Eng. Res. Des.* **2000**, *78*, 943–946, DOI: 10.1205/026387600528193
69. Melian-Cabrera, O.; Granados M.L. ; Terreros, P.; Fierro, J.L.G. CO 2 hydrogenation over Pd-modified methanol synthesis catalysts *Catal. Today* **1998**, *45*, 251–256, DOI: 10.1016/S0920-5861(98)00224-7
70. Ban, H.; Li, C.; Asami, K.; Fujimoto, K. Influence of rare-earth elements (La, Ce, Nd and Pr) on the performance of Cu/Zn/Zr catalyst for CH 3 OH synthesis from CO 2. *Catal. Commun.* **2014**, *54*, 50–54, DOI: 10.1016/j.catcom.2014.05.014
71. Guo, X.; Mao, D.; Lu, G.; Wang, S.; Wu, G. The influence of La doping on the catalytic behavior of Cu/ZrO 2 for methanol synthesis from CO 2 hydrogenation. *J. Mol. Catal. A* **2011**, *345*, 60–68, DOI: 10.1016/j.molcata.2011.05.019
72. Batyrev, E.D.; van den Heuvel, J.C., Beckers, J.; Jansen, W.P.A.; Castricum, H.L. The effect of the reduction temperature on the structure of Cu/ZnO/SiO 2 catalysts for methanol synthesis. *J. Catal.* **2005**, *229*, 136–143, DOI: 10.1016/j.jcat.2004.10.012
73. Owen, G.; Hawkes C.M.; Lloyd, D. Methanol synthesis from intermetallic precursors: binary lanthanide-copper catalysts. *Appl. Catal.* **1987**, *33*, 405-430. DOI: 10.1016/S0166-9834(00)83071-7
74. Bonura, G.; Arena, F.; Mezzatesta, G.; Cannilla, C.; Spadaro, L.; Frusteri, F. Role of the ceria promoter and carrier on the functionality of Cu-based catalysts in the CO 2-to-methanol hydrogenation reaction. *Catal. Today* **2011**, *171*, 251–256, DOI: 10.1016/j.cattod.2011.04.038
75. Meng-Jung Li, M.; Zeng, Z.; Liao, F.; Hong, X.; Tsang, S.C.E. Enhanced CO 2 hydrogenation to methanol over CuZn nanoalloy in Ga modified Cu/ZnO catalysts. *J. Catal.* **2016**, *343*, 157–167, DOI: 10.1016/j.jcat.2016.03.020
76. Toyir, J.; Ramìrez de la Piscina, P.; Homs, N. Ga-promoted copper-based catalysts highly selective for methanol steam reforming to hydrogen; relation with the hydrogenation of CO 2 to methanol. *Int. J. Hydrogen Energy* **2015**, *40*, 11261–11266, DOI: 10.1016/j.ijhydene.2015.04.039
77. Zhang, Y.; Li, D.; Zhang, Y.; Cao, Y.; Zhang, S.; Wang, K.; Ding, F.; Wu, J. V-modified CuO–ZnO–ZrO 2/HZSM-5 catalyst for efficient direct synthesis of DME from CO 2 hydrogenation. *Catal. Commun.* **2014**, *55*, 49–52, DOI: 10.1016/j.catcom.2014.05.026
78. Zhang, Q.; Zuo, Y.-Z.; Han, M.-H.; Wang, J.-F.; Jin, Y.; Wei, F. Long carbon nanotubes intercrossed Cu/Zn/Al/Zr catalyst for CO/CO 2 hydrogenation to methanol/dimethyl ether. *Catal. Today* **2010**, *150*, 55–60, DOI: 10.1016/j.cattod.2009.05.018
79. Deerattrakul, V.; Dittanet, P.; Sawangphruk, M.; Kongkachuichay, P. CO 2 hydrogenation to methanol using Cu-Zn catalyst supported on reduced graphene oxide nanosheets. *J. CO2 Util.* **2016**, *16*, 104–113, DOI: 10.1016/j.jcou.2016.07.002
80. Fan, Y.J.; Wu, S.F. A graphene-supported copper-based catalyst for the hydrogenation of carbon dioxide to form methanol. *J. CO2 Util.* **2016**, *16*, 150–156, DOI: 10.1016/j.jcou.2016.07.001
81. Ahmed, N.; Shibata, Y.; Taniguchi, T.; Izumi, Y. Photocatalytic conversion of carbon dioxide into methanol using zinc–copper–M (III)(M= aluminum, gallium) layered double hydroxides. *J. Catal.* **2011**, *279*, 123–135, DOI: 10.1016/j.jcat.2011.01.004
82. Wang, G.; Zuo, Y.; Han, M.; Wang, J. Copper crystallite size and methanol synthesis catalytic property of Cu-based catalysts promoted by Al, Zr and Mn. *React. Kinet. Mech. Catal.* **2010**, *101*, 443–454, DOI: 10.1007/s11144-010-0240-9

83. Ladera, R.; Pérez-Alonso, F.J.; González-Carballo, J.M.; Ojeda, M.; Rojas, S.; Fierro, J.L.G. Catalytic valorization of CO2 via methanol synthesis with Ga-promoted Cu–ZnO–ZrO 2 catalysts. *Appl. Catal. B* **2013**, *142–143*, 241–248, DOI: 10.1016/j.apcatb.2013.05.019
84. Zhan, H.; Li, F.; Xin, C.; Zhao, N.; Xiao, F.; Wei, W.; Sun, Y. Performance of the La–Mn–Zn–Cu–O Based Perovskite Precursors for Methanol Synthesis from CO2 Hydrogenation. *Catal. Lett.* **2015**, *145*, 1177–1185, DOI: 10.1007/s10562-015-1513-8
85. Azizi, Z.; Rezaeimanesh, M.; Tohidian, T.; Rahimpour, M.R. Dimethyl ether: A review of technologies and production challenges. *Chem. Eng. Process.* **2014**, *82*, 150–172, DOI: 10.1016/j.cep.2014.06.007
86. Tavan, Y.; Hosseini, S.H.; Ghavipour, M.; Nikou, M.R.K.; Shariati, A. From laboratory experiments to simulation studies of methanol dehydration to produce dimethyl ether—Part I: Reaction kinetic study. *Chem. Eng. Process.* **2013**, *73*, 144–150, DOI: 10.1016/j.cep.2013.06.006
87. Khaleel, A. Titanium-doped alumina for catalytic dehydration of methanol to dimethyl ether at relatively low temperatures *Fuel* **2011**, *90*, 2422 – 2427, DOI: 10.1016/j.fuel.2011.03.008
88. Liu, D.; Yao, C.; Zhang, J.; Fan, D.; Chen, D. Catalytic dehydration of methanol to dimethyl ether over modified γ-Al 2 O 3 catalyst *Fuel* **2011**, *90*, 1738 – 1742, DOI: 10.1016/j.fuel.2011.01.038
89. Mollavalli, M.; Yaripour, F.; Mohammadi-Jam, Sh.; Atashi, H. Relationship between surface acidity and activity of solid-acid catalysts in vapour phase dehydration of methanol. *Fuel Process. Technol.* **2009**, *90*, 1093–1098, DOI: 10.1016/j.fuproc.2009.04.018
90. Xia, J.; Mao, D.; Zhang, B.; Chen, Q.; Zhang, Y.; Tang, Y. Catalytic properties of fluorinated alumina for the production of dimethyl ether. *Catal. Comm.* **2006**, *7*, 362–366, DOI: 10.1016/j.catcom.2005.12.011
91. Yaripour, F.; Shariatinia, Z.; Sahebdelfar, S.; Irandoukht, A. The effects of synthesis operation conditions on the properties of modified γ-alumina nanocatalysts in methanol dehydration to dimethyl ether using factorial experimental design. *Fuel* **2015**, *139*, 40–50, DOI: 10.1016/j.fuel.2014.08.029
92. Xu, M.; Lunsford, J.H.; Goodman, D.W.; Bhattacharyya, A. Synthesis of dimethyl ether (DME) from methanol over solid-acid catalysts. *Appl. Catal. A* **1997**, *149*, 289–301, DOI: 10.1016/S0926-860X(96)00275-X
93. Yaripour, F.; Baghaei, F.; Schmidt, I.; Perregaard J. Catalytic dehydration of methanol to dimethyl ether (DME) over solid-acid catalysts. *Catal. Commun.* **2005**, *6*, 147–152, DOI: 10.1016/j.catcom.2004.11.012
94. Jun, K.W., Lee, H.S.; Roh, H.S.; Park, S.E. Highly water-enhanced H-ZSM-5 catalysts for dehydration of methanol to dimethyl ether. *Bull. Korean Chem. Soc.* **2003**, *24*, 106–108.
95. Tao, J.; Jun, K.; Lee, K. Co-production of dimethyl ether and methanol from CO2 hydrogenation: development of a stable hybrid catalyst. *Appl. Organomet. Chem.* **2001**, *15*, 105–108.
96. Alharbi, W.; Kozhevnikova, E.F.; Kozhevnikov I.V. Dehydration of methanol to dimethyl ether over heteropoly acid catalysts: the relationship between reaction rate and catalyst acid strength. *ACS Catal.* **2015**, *5*, 7186–7193, DOI: 10.1021/acscatal.5b01911
97. Ladera, R.M.; Fierro, J.L.G.; Ojeda, M.; Rojas, S. TiO 2-supported heteropoly acids for low-temperature synthesis of dimethyl ether from methanol. *J. Catal.* **2014**, *312*, 195–203, DOI: 10.1016/j.jcat.2014.01.016
98. Spivey, J. Review: dehydration catalysts for the methanol/dimethyl ether reaction, *Chem. Eng. Comm.* **1991**, *110*, 123–142.
99. Ciftci, A.; Sezgi, N.A.; Dogu, T. Nafion-incorporated silicate structured nanocomposite mesoporous catalysts for dimethyl ether synthesis. *Ind. Eng. Chem. Res.* **2010**, *49*, 6753–6762, DOI: 10.1021/ie901566
100. Varisli, D.; Dogu, T. Production of clean transportation duel dimethylether by dehydration of methanol over nafion catalyst. *Gazi University J. Sci.* **2008**, *1*, 37–41.
101. Hosseininejad, S.; Afacan, A.; Hayes, R.E. Catalytic and kinetic study of methanol dehydration to dimethyl ether. *Chem. Eng. Res. Des.* **2012**, *90*, 825–833, DOI: 10.1016/j.cherd.2011.10.007
102. Harmer, M.A.; Sun, Q. Solid acid catalysis using ion-exchange resins. *Appl. Catal. A* **2001**, *221*, 45–62, DOI: 10.1016/S0926-860X(01)00794-3
103. Frontera, P.; Macario, A.; Aloise, A.; Crea, F.; Antonucci, P.L.; B.Nagy, J.; Frusteri, F.; Giordano, G. Catalytic dry-reforming on Ni–zeolite supported catalyst. *Catal. Today* **2012**, *179*, 52-60, DOI: 10.1016/j.cattod.2011.07.039
104. Frontera, P.; Macario, A.; Aloise, A.; Antonucci, P.L.; Giordano, G.; B.Nagy, J. Effect of support surface on methane dry-reforming catalyst preparation. *Catal. Today* **2013**, *218*, 18-29, DOI: 10.1016/j.cattod.2013.04.029
105. Frontera, P.; Aloise, A.; Macario, A.; Antonucci, P.L.; Crea, F., Giordano, G.; B.Nagy, J. Bimetallic zeolite catalyst for CO2 reforming of methane. *Top. Catal.* **2010**, *53*, 265-272, DOI: 10.1007/s11244-009-9409-8

106. Macario, A.; Giordano, G. Catalytic conversion of renewable sources for biodiesel production: a comparison between biocatalysts and inorganic catalysts. *Catal. Lett.* **2013**, *143*, 159-168, DOI: 10.1007/s10562-012-0949-3
107. Macario, A.; Verri, F.; Diaz, U.; Corma, A.; Giordano, G. Pure silica nanoparticles for liposome/lipase system encapsulation: Application in biodiesel production. *Catal. Today* **2013**, *204*, 148-155, DOI: 10.1016/j.cattod.2012.07.014
108. Corma, A. State of the art and future challenges of zeolites as catalysts. *J. Catal.* **2003**, *216*, 298–312, DOI: 10.1016/S0021-9517(02)00132-X
109. Vishwanathan, V.; Jun, K.; Kim, J.; Roh, H. Vapour phase dehydration of crude methanol to dimethyl ether over Na-modified H-ZSM-5 catalysts. *Appl. Catal. A* **2005**, *276*, 251–255, DOI: 10.1016/j.apcata.2004.08.011
110. Migliori, M.; Aloise, A.; Catizzone, E.; Giordano, G. Kinetic analysis of methanol to dimethyl ether reaction over H-MFI catalyst. *Ind. Eng. Chem. Res.* **2014**, *53*, 14885–14891, DOI: 10.1021/ie502775u
111. Andzelm, J.; Goving, N.; Fitzgerald, G., Maiti, A. DFT study of methanol conversion to hydrocarbons in a zeolite catalyst. *Int. J. Quantum Chem.* **2003**, *91*, 467–473, DOI: 10.1002/qua.10417
112. Wang, W.; Seiler, M.; Hunger, M. Role of surface methoxy species in the conversion of methanol to dimethyl ether on acidic zeolites investigated by in situ stopped-flow MAS NMR spectroscopy. *J. Phys. Chem. B* **2001**, *105*, 12553–12558, DOI: 10.1021/jp0129784.
113. Migliori, M.; Aloise, A.; Giordano, G. Methanol to dimethylether on H-MFI catalyst: The influence of the Si/Al ratio on kinetic parameters. *Catal. Today* **2014**, *227*, 138–143, DOI: 10.1016/j.cattod.2013.09.033
114. Tajima, N.; Tsuneda, T.; Toyama, F.; Hirao, K. A new mechanism for the first carbon− carbon bond formation in the MTG process: a theoretical study. *J. Am. Chem. Soc.* **1998**, *120*, 8222–8229, DOI: 10.1021/ja9741483
115. Teketel, S.; Olsbye, U.; Lillerud, K.P.; Beato, P.; Svelle, S. Co-conversion of methanol and light alkenes over acidic zeolite catalyst H-ZSM-22: Simulated recycle of non-gasoline range products. *Appl. Catal. A* **2015**, *494*, 68–76, DOI: 10.1016/j.apcata.2015.01.035
116. Li, J.; Wei Z.; Chen, Y.; Jing, B.; He, Y.; Dong, M.; Jiao, H.; Li, X.; Qin, Z.; Wang, J.; Fan, W. A route to form initial hydrocarbon pool species in methanol conversion to olefins over zeolites. *J. Catal.* **2014**, *317*, 277–283, DOI: 10.1016/j.jcat.2014.05.015
117. Qi, L.; Wei, Y.; Xu, L.; Liu, Z. Reaction behaviors and kinetics during induction period of methanol conversion on HZSM-5 zeolite. *ACS Catal.* **2015**, *5*, 3973–3982, DOI: 10.1021/acscatal.5b00654
118. Svelle, S., Joensen, F.; Nerlov, J.; Olsbye, U.; Lillerud, K.P.; Kolboe, S.; Bjørgen, M. Conversion of methanol into hydrocarbons over zeolite H-ZSM-5: Ethene formation is mechanistically separated from the formation of higher alkenes. *J. Am. Chem. Soc.* **2006**, *128*, 14770-14771, DOI: 10.1021/ja065810a
119. Campelo, J.M.; Lafont, F.; Marinas, J.M., Ojeda, M. Studies of catalyst deactivation in methanol conversion with high, medium and small pore silicoaluminophosphates. *Appl. Catal. A* **2000**, *192*, 85–96, DOI: 10.1016/S0926-860X(99)00329-4
120. Palumbo, L.; Bonino, F.; Beato, P.; Bjørgen, M.; Zecchina, A.; Bordiga, S. Conversion of methanol to hydrocarbons: spectroscopic characterization of carbonaceous species formed over H-ZSM-5. *J. Phys. Chem. C* **2008**, *112*, 9710–9716, DOI: 10.1021/jp800762v
121. Chua, Y.T.; Stair, P.C. An ultraviolet Raman spectroscopic study of coke formation in methanol to hydrocarbons conversion over zeolite H-MFI. *J. Catal.* **2003**, *213*, 39–46, DOI: 10.1016/S0021-9517(02)00026-X
122. Mentzel, U.V.; Hojholt, K.; Holm, M.S.; Fehrmann, R., Beato, P. Conversion of methanol to hydrocarbons over conventional and mesoporous H-ZSM-5 and H-Ga-MFI: Major differences in deactivation behavior. *Appl. Catal. A* **2012**, *417–418*, 290–297, DOI: 10.1016/j.apcata.2012.01.003
123. Nushyama, N.; Kawaguchi, M.; Hirota, Y.; Van Vu, D.; Egashira, Y.; Ueyama, K. Size control of SAPO-34 crystals and their catalyst lifetime in the methanol-to-olefin reaction. *Appl. Catal. A* **2009**, *362*, 193–199, DOI:
124. Deimund, M.A.; Schmidt, J.E.; Davis, M.E. *Top. Catal.* **2015**, *58*, 416–423, DOI: 10.1016/j.apcata.2009.04.044
125. Catizzone, E.; Aloise, A.; Migliori, M.; Giordano, G. From 1-D to 3-D zeolite structures: performance assessment in catalysis of vapour-phase methanol dehydration to DME. *Microp. Mesop. Mater.* **2017**, *243*, 102–111, DOI: 10.1016/j.micromeso.2017.02.022
126. Catizzone, E.; Aloise, A.; Migliori, M. Dimethyl ether synthesis via methanol dehydration: Effect of zeolite structure. *Appl. Catal. A* **2015**, *502*, 215–220, DOI: 10.1016/j.apcata.2015.06.017

127. Khandan, N.; Kazemeini, M.; Aghaziarati, M. Determining an optimum catalyst for liquid-phase dehydration of methanol to dimethyl ether. *Appl. Catal. A* **2008**, *349*, 6–12, DOI: 10.1016/j.apcata.2008.07.029
128. Tang, Q.; Xu, H.; Zheng, Y.; Wang, J.; Li, H.; Zhang, J. Catalytic dehydration of methanol to dimethyl ether over micro–mesoporous ZSM-5/MCM-41 composite molecular sieves. *Appl. Catal. A* **2012**, *413–414*, 36–42, DOI: 10.1016/j.apcata.2011.10.039
129. Rutkowska, M.; Macina, D.; Piwowarska, Z.; Gajewska, M.; Diaz, U.; Chmielarz, L. Hierarchically structured ZSM-5 obtained by optimized mesotemplate-free method as active catalyst for methanol to DME conversion. *Catal. Sci. Technol.* **2016**, *6*, 4849–4862, DOI: 10.1039/C6CY00040A
130. Baek, S.-C.; Lee, Y.-J.; Jun, K.-W.; Hong, S.B. Influence of catalytic functionalities of zeolites on product selectivities in methanol conversion. *Energy Fuels* **2009**, *23*, 593–598, DOI: 10.1021/ef800736n
131. Catizzone, E.; Aloise, A.; Migliori, M.; Giordano, G. The effect of FER zeolite acid sites in methanol-to-dimethyl-ether catalytic dehydration. *J. Energy Chem*. **2017**, *26*, 406–415, DOI: 10.1016/j.jechem.2016.12.005
132. Kim, S.D.; Baek, S.C.; Lee, Y.; Jun, K.; Kim, M.J.; Yoo, I.S. Effect of γ-alumina content on catalytic performance of modified ZSM-5 for dehydration of crude methanol to dimethyl ether. *Appl. Catal. A* **2006**, *309*, 139–143, DOI: doi.org/10.1016/j.apcata.2006.05.008
133. Hassanpour, S.; Yaripour, F.; Taghizadeh, M. Performance of modified H-ZSM-5 zeolite for dehydration of methanol to dimethyl ether. *Fuel Process. Technol*. **2010**, *91*, 1212–1221, DOI: 10.1016/j.fuproc.2010.03.035
134. Khandan, N.; Kazemeini, M.; Aghaziarati, M. Dehydration of methanol to dimethyl ether employing modified H-ZSM-5 catalysts. *Iran. J. Chem. Eng.* **2009**, *6*, 3–1, DOI:
135. Hassanpour, S.; Taghizadeh, M.; Yaripour, F. Preparation, characterization, and activity evaluation of H-ZSM-5 catalysts in vapor-phase methanol dehydration to dimethyl ether. *Ind. Eng. Chem. Res.* **2010**, *49*, 4063–4069, DOI: 10.1021/ie9013869
136. Amaroli, T.; Simon, L.J.; Digne, M.; Montanari, T.; Bevilacqua, M.; Valtchev, V.; Patarin, J.; Busca, G. Effect of crystal size and Si/Al ratio on the surface properties of H-ZSM-5 zeolites. *Appl. Catal. A* **2006**, *306*, 78–84, DOI: 0.1016/j.apcata.2006.03.030
137. García-Trenco, A.; Martínez, A. Direct synthesis of DME from syngas on hybrid CuZnAl/ZSM-5 catalysts: New insights into the role of zeolite acidity. *Appl. Catal. A* **2012**, *411–412*, 170–179, DOI: 10.1016/j.apcata.2011.10.036
138. Frusteri, F.; Cordaro, M.; Cannilla, C.; Bonura, "Multifunctionality of Cu–ZnO–ZrO 2/H-ZSM5 catalysts for the one-step CO 2-to-DME hydrogenation reaction. *Appl. Catal. B* **2015**, *162*, 57–65, DOI: 10.1016/j.apcatb.2014.06.035
139. Wang, D.; Han, Y.; Tan, Y.; Tsubaki, N. Effect of H 2 O on Cu-based catalyst in one-step slurry phase dimethyl ether synthesis. *Fuel Process. Technol.* **2009**, *90*, 446–451, DOI: 10.1016/j.fuproc.2008.11.007.
140. Diban, N.; Urtiaga, A.M.; Ortiz, I.; Ereña, J.; Bilbao, J.; Aguayo, A.T. Influence of the membrane properties on the catalytic production of dimethyl ether with in situ water removal for the successful capture of CO 2. *Chem. Eng. J.* **2013**, *234*, 140–148, DOI: 10.1016/j.cej.2013.08.062
141. Iliuta, I., Larachi, F.; Fongarland, P. Dimethyl ether synthesis with in situ H2O removal in fixed-bed membrane reactor: model and simulations. *Ind. Eng. Chem. Res.* **2010**, *49*, 6870–6877, DOI: 10.1021/ie901726u
142. Haw, J.F.; Song, W.; Marcus, D.M.; Nicholas, J.B. The mechanism of methanol to hydrocarbon catalysis. *Acc. Chem. Res.* **2003**, *36*, 317–326, DOI: 10.1021/ar020006o
143. Stich, I.; Gale, J.D., Terakura, K.; Payne, M.C. Role of the zeolitic environment in catalytic activation of methanol. *J. Am. Chem. Soc.* **1999**, *121*, 3292–3302, DOI: 10.1021/ja983470q
144. Ivanova, S.; Lebrun, C.; Vanhaecke, E.; Pham-Huu, C.; Louis, B. Influence of the zeolite synthesis route on its catalytic properties in the methanol to olefin reaction. *J. Catal.* **2009**, *265*, 1–7, DOI: 10.1016/j.jcat.2009.03.016
145. Naik, S.P.; Ryu, T.; Bui, V.; Miller, J.D.; Drinnan, N.B.; Zmierczak, W. Synthesis of DME from CO 2/H 2 gas mixture. *Chem. Eng. J.* **2011**, *167*, 362–368, DOI: 10.1016/j.cej.2010.12.087
146. Zhao, Y.; Chen, J.; Zhang, J. Effects of ZrO2 on the performance of CuO-ZnO-Al2O3/HZSM-5 catalyst for dimethyl ether synthesis from CO2 hydrogenation. *J. Nat. Gas. Chem.* **2007**, *16*, 389–392, DOI: 10.1016/S1003-9953(08)60009-2
147. Park, Y.; Baek, S.; Ihm, S. CO2 hydrogenation over copper-based hybrid catalysts for the synthesis of oxygenates *Fuel Chem. Div. Prep.* **2002**, *47*, 293–294.

148. Ereña, J.; Garona, R.; Arandes, J.M.; Aguayo, A.T.; Bilbao, J. Effect of operating conditions on the synthesis of dimethyl ether over a CuO-ZnO-Al 2 O 3/NaHZSM-5 bifunctional catalyst. *Catal. Today* **2005**, *107–108*, 467–473, DOI: 10.1016/j.cattod.2005.07.116
149. Wang, S.; Mao, D.; Guo, X.; Wu, X.; Lu, G. Dimethyl ether synthesis via CO 2 hydrogenation over CuO–TiO 2–ZrO 2/HZSM-5 bifunctional catalysts. *Catal. Commun.* **2009**, *10*, 1367–1370, DOI: 10.1016/j.catcom.2009.02.001
150. Gao, W.; Wang, H.; Wang, Y.; Guo, W.; Jia, M. Dimethyl ether synthesis from CO2 hydrogenation on La-modified CuO-ZnO-Al2O3/HZSM-5 bifunctional catalysts *J. Rare Earths* **2013**, *31*, 470–476, DOI: 10.1016/S1002-0721(12)60305-6
151. Qi, G.X.; Fei, J.H.; Zheng, X.M.; Hou, Z.Y. DME synthesis from carbon dioxide and hydrogen over Cu–Mo/HZSM-5. *Catal. Lett.* **2001**, *72*, 121–124.
152. Sun, K.; Lu, W.; Wang, M., Xu, X. Low-temperature synthesis of DME from CO 2/H 2 over Pd-modified CuO–ZnO–Al 2 O 3–ZrO 2/HZSM-5 catalysts. *Catal. Commun.* **2004**, *5*, 367–370, DOI: 10.1016/j.catcom.2004.03.012
153. Zha, F.; Tian, H.; Yan, J.; Chang, Y. Multi-walled carbon nanotubes as catalyst promoter for dimethyl ether synthesis from CO 2 hydrogenation. *Appl. Surf. Sci.* **2013**, *285*, 945–951, DOI: 10.1016/j.apsusc.2013.06.150.
154. Bonura, G.; Cannilla, C.; Frusteri, L.; Mezzapica, A.; Frusteri, F. DME production by CO 2 hydrogenation: Key factors affecting the behaviour of CuZnZr/ferrierite catalysts. *Catal. Today* **2017**, *281*, 337–344, DOI: 10.1016/j.cattod.2016.05.057
155. Ereña, J.; Garoña, R., Arandes, J.M., Aguayo, A.T.; Bilbao, J. Direct synthesis of dimethyl ether from (H2+ CO) and (H2+ CO2) feeds. Effect of feed composition. *Int. J. Chem. React. Eng.* **2005**, *3*, 1–15, DOI: 10.2202/1542-6580.1295
156. Zha, F.; Ding, J.; Chang, Y.; Ding, J.; Wang, J.; Ma, J. Cu–Zn–Al Oxide Cores Packed by Metal-Doped Amorphous Silica–Alumina Membrane for Catalyzing the Hydrogenation of Carbon Dioxide to Dimethyl Ether. *Ind. Eng. Chem. Res.* **2012**, *51*, 345–352, DOI: 10.1021/ie202090f
157. Liu, R.; Qin, Z.; Ji, H.; Su, T. Synthesis of dimethyl ether from CO2 and H2 using a Cu–Fe–Zr/HZSM-5 catalyst system. *Ind. Eng. Chem. Res.* **2013**, *52*, 16648–16655, DOI: 10.1021/ie401763g
158. Frusteri, F.; Migliori, M.; Cannilla, C.; Frusteri, L.; Catizzone, E.; Aloise, A.; Giordano, G.; Bonura, G. Direct CO2-to-DME hydrogenation reaction: new evidences of a asuperiori behvaiour of FER-based hybrid systems to obtain high DME yield *J. CO2 Util.* **2017**, *18*, 353–361, DOI: 10.1016/j.jcou.2017.01.030
159. Allahyari S.; Haghighi M.; Ebadi A.; Hosseinzadeh, S. Effect of irradiation power and time on ultrasound assisted co-precipitation of nanostructured CuO–ZnO–Al 2 O 3 over HZSM-5 used for direct conversion of syngas to DME as a green fuel. *Energy Conv. Manag.* **2014**, *83*, 212–222, DOI: 10.1016/j.enconman.2014.03.071
160. Bonura, G.; Frusteri, F.; Cannilla, C.; Drago Ferrante, G.; Aloise, A.; Catizzone, E.; Migliori, M.; Giordano, G. Catalytic features of CuZnZr–zeolite hybrid systems for the direct CO 2-to-DME hydrogenation reaction. *Catal. Today* **2016**, *277*, 48–54, DOI: 10.1016/j.cattod.2016.02.013
161. Frusteri, F.; Bonura, G.; Cannilla, C.; Drago Ferrante, G.; Aloise, A.; Catizzone, E.; Migliori, M.; Giordano, G. Stepwise tuning of metal-oxide and acid sites of CuZnZr-MFI hybrid catalysts for the direct DME synthesis by CO 2 hydrogenation. *Appl. Catal. B* **2015**, *176*, 522–531, DOI: 10.1016/j.apcatb.2015.04.032
162. Bansode, A.; Urakawa A. Towards full one-pass conversion of carbon dioxide to methanol and methanol-derived products. *J. Catal.* **2014**, *309*, 66-70, DOI: 10.1016/j.jcat.2013.09.005
163. Bae, J.W.; Kang, S.-H.; Lee, Y.-J.; Jun, K.-W. Effect of precipitants during the preparation of Cu-ZnO-Al 2 O 3/Zr-ferrierite catalyst on the DME synthesis from syngas. *J. Ind. Eng. Chem.* **2009**, *15*, 566–572, DOI: 10.1016/j.jiec.2009.01.014
164. Yang, G.; Tsubaki, N.; Shamoto, J.; Yoneyama, Y.; Zhang, Y. Confinement effect and synergistic function of H-ZSM-5/Cu-ZnO-Al2O3 capsule catalyst for one-step controlled synthesis. *J. Am. Chem. Soc.* **2010**, *132*, 8129–8136, DOI: 10.1021/ja101882a
165. Yang, G.; Thongkam, M.; Vitidsant, T.; Yoneyama, Y.; Tan, Y.; Tsubaki, N. A double-shell capsule catalyst with core–shell-like structure for one-step exactly controlled synthesis of dimethyl ether from CO 2 containing syngas. *Catal. Today* **2011**, *171*, 229–235, DOI: 10.1016/j.cattod.2011.02.021
166. Nie, R.; Lei, H.; Pan, S.; Wang, L.; Fei, J.; Hou, Z. Core–shell structured CuO–ZnO@ H-ZSM-5 catalysts for CO hydrogenation to dimethyl ether *Fuel* **2012**, *96*, 419–425, DOI: 10.1016/j.fuel.2011.12.048
167. Sun, K.; Lu, W.; Qiu, F.; Liu, S.; Xu, X. Direct synthesis of DME over bifunctional catalyst: surface properties and catalytic performance. *Appl. Catal. A* **2003**, *252*, 243–249, DOI: 10.1016/S0926-860X(03)00466-6

168. García-Trenco, A.; Vidal-Moya, A.; Martínez, A. Study of the interaction between components in hybrid CuZnAl/HZSM-5 catalysts and its impact in the syngas-to-DME reaction. *Catal. Today* **2012**, *179*, 43–51, DOI: 10.1016/j.cattod.2011.06.034
169. Jin, D.; Zhu, B.; Hou, Z., Fei, J.; Lou, H.; Zheng, X. Dimethyl ether synthesis via methanol and syngas over rare earth metals modified zeolite Y and dual Cu–Mn–Zn catalysts. *Fuel* **2007**, *86*, 2707–2713, DOI: 10.1016/j.fuel.2007.03.011
170. Stiefel, M.; Ahmad, R.; Amold, U.; Döring, M. Direct synthesis of dimethyl ether from carbon-monoxide-rich synthesis gas: influence of dehydration catalysts and operating conditions. *Fuel Process. Technol.* **2011**, *92*, 1466–1474, DOI: 10.1016/j.fuproc.2011.03.007
171. Chen, H.-J.; Fan, C.-W.; Yu, C.-S. Analysis, synthesis, and design of a one-step dimethyl ether production via a thermodynamic approach. *Appl. Energy* **2013**, *101*, 449–456, DOI: 10.1016/j.apenergy.2012.08.025
172. Moradi, G.R.; Yaripour, F.; Vale-Sheyda, P. Catalytic dehydration of methanol to dimethyl ether over mordenite catalysts. *Fuel Process. Technol.* **2010**, *91*, 461–468, DOI: 10.1016/j.fuproc.2009.12.005
173. Chen, W.-H; Lin, B.-J.; Lee, H.-M.; Huang, M.-H. ne-step synthesis of dimethyl ether from the gas mixture containing CO 2 with high space velocity. *Appl. Energy* **2012**, *98*, 92–101, DOI: 10.1016/j.apenergy.2012.02.082
174. Rownaghi, A.; Rezaei, F.; Stante, M.; Hedlund, J. Selective dehydration of methanol to dimethyl ether on ZSM-5 nanocrystals. *Appl. Catal. B* **2012**, *119*, 56–61, DOI: 10.1016/j.apcatb.2012.02.017
175. Raoof, F.; Taghizadeh, M.; Eliassi, A.; Yaripour, F. Effects of temperature and feed composition on catalytic dehydration of methanol to dimethyl ether over γ-alumina. *Fuel* **2008**, *87*, 2967–2971, DOI: 10.1016/j.fuel.2008.03.025